The Astrophysical Journal Supplement Series, 217:2 (26pp), 2015 March doi:10.1088/0067-0049/217/1/2

REFINING THE ASSOCIATIONS OF THE *FERMI* LARGE AREA TELESCOPE SOURCE CATALOGS

F. Massaro[1,2], R. D'Abrusco[3], M. Landoni[4], A. Paggi[3], N. Masetti[5], M. Giroletti[6], H. Otí-Floranes[7,8], V. Chavushyan[9], E. Jiménez-Bailón[7], V. Patiño-Álvarez[9], S. W. Digel[10], Howard A. Smith[3], and G. Tosti[11]
[1] Dipartimento di Fisica, Università degli Studi di Torino, via Pietro Giuria 1, I-10125 Torino, Italy
[2] Yale Center for Astronomy and Astrophysics, Physics Department, Yale University, P.O. Box 208120, New Haven, CT 06520-8120, USA
[3] Harvard-Smithsonian Astrophysical Observatory, Center for Astrophysics, 60 Garden Street, Cambridge, MA 02138, USA
[4] INAF-Osservatorio Astronomico di Brera, Via Emilio Bianchi 46, I-23807 Merate, Italy
[5] INAF-Istituto di Astrofisica Spaziale e Fisica Cosmica di Bologna, via Gobetti 101, I-40129, Bologna, Italy
[6] INAF Istituto di Radioastronomia, via Gobetti 101, I-40129, Bologna, Italy
[7] Instituto de Astronomía, Universidad Nacional Autónoma de México, Apdo. Postal 877, Ensenada, 22800 Baja California, México
[8] Centro de Radioastronomía and Astrofísica, UNAM, Campus Morelia, México
[9] Instituto Nacional de Astrofísica, Óptica y Electrónica, Apartado Postal 51-216, 72000 Puebla, México
[10] SLAC National Accelerator Laboratory and Kavli Institute for Particle Astrophysics and Cosmology, 2575 Sand Hill Road, Menlo Park, CA 94025, USA
[11] Dipartimento di Fisica, Università degli Studi di Perugia, I-06123 Perugia, Italy
Received 2014 October 6; accepted 2014 November 22; published 2015 February 26

ABSTRACT

The *Fermi*-Large Area Telescope (LAT) First Source Catalog (1FGL) was released in 2010 February and the *Fermi*-LAT 2-Year Source Catalog (2FGL) appeared in 2012 April, based on data from 24 months of operation. Since they were released, many follow up observations of unidentified γ-ray sources have been performed and new procedures for associating γ-ray sources with potential counterparts at other wavelengths have been developed. Here we review and characterize all of the associations as published in the 1FGL and 2FGL catalogs on the basis of multifrequency archival observations. In particular, we located 177 spectra for the low-energy counterparts that were not listed in the previous *Fermi* catalogs, and in addition we present new spectroscopic observations of eight γ-ray blazar candidates. Based on our investigations, we introduce a new counterpart category of "candidate associations" and propose a refined classification for the candidate low-energy counterparts of the *Fermi* sources. We compare the 1FGL-assigned counterparts with those listed in 2FGL to determine which unassociated sources became associated in later releases of the *Fermi* catalogs. We also search for potential counterparts to all of the remaining unassociated *Fermi* sources. Finally, we prepare a refined and merged list of all of the associations of 1FGL plus 2FGL that includes 2219 unique *Fermi* objects. This is the most comprehensive and systematic study of all the associations collected for the γ-ray sources available to date. We conclude that 80% of the *Fermi* sources have at least one known plausible γ-ray emitter within their positional uncertainty regions.

Key words: galaxies: active – methods: statistical – quasars: general – surveys

Supporting material: machine-readable table

1. INTRODUCTION

Despite the large progress in γ-ray source localization made by the *Fermi* Large Area Telescope (LAT; Atwood et al. 2009), coupled with improvements in our knowledge of the diffuse Galactic γ-ray emission (e.g., Moskalenko et al. 2007; Abdo et al. 2009), the positional uncertainties of the *Fermi* sources are still large with respect to typical localization precisions at X-ray and lower energies, making a significant fraction of the sources in the γ-ray sky still unknown (Abdo et al. 2010a; Nolan et al. 2012). About 43% of the *Fermi* sources detected in the *Fermi*-LAT First Source Catalog (1FGL; Abdo et al. 2010a) were listed as UGSs, while there were ∼33% γ-ray objects unassociated in the *Fermi*-LAT 2-Year Source Catalog (2FGL, Nolan et al. 2012).

To decrease the number of unidentified γ-ray sources (UGSs), many methods based on multifrequency approaches or statistical analyses have recently been adopted. Radio follow up observations of the *Fermi* UGSs have already been performed (e.g., Kovalev 2009; Hovatta et al. 2012, 2014; Petrov et al. 2013; Schinzel et al. 2014) and the *Swift* X-ray survey for all the UGSs listed in the *Fermi* source catalogs is still on going[12] (e.g., Mirabal & Halpern 2009; Acero et al. 2013; Paggi et al. 2013; Cowperthwaite et al. 2013; Stroh & Falcone 2013; Takeuchi et al. 2013). Additional X-ray observations performed with *Chandra* and *Suzaku* have improved our knowledge of UGSs (e.g., Maeda et al. 2011; Cheung et al. 2012; Kataoka et al. 2012; Takahashi et al. 2012). Statistical studies based on γ-ray source properties have also allowed us to recognize the nature of the potential counterparts for UGSs (e.g., Ackermann et al. 2012; Mirabal et al. 2012; Hassan et al. 2013; Doert & Errando 2014). Moreover, a tight connection between the infrared (IR) sky seen by the Wide-Field Infrared Survey Explorer (WISE, Wright et al. 2010) and that of *Fermi* one has recently been discovered for blazars, the rarest class of active galaxies (Massaro et al. 2011a; D'Abrusco et al. 2012, 2013). These works greatly decreased the fraction of UGSs with no assigned counterpart at low energies (Massaro et al. 2012a, 2012b, 2013a). More recently, low frequency radio observations (i.e., below ∼1 GHz) also revealed new spectral behavior that has allowed us to search for blazar-like sources lying within the positional uncertainty regions of UGSs (Massaro et al. 2013b; Nori et al. 2014). Additional studies have been also carried out with near-IR observations (Raiteri et al. 2014) as well as in the submillimeter range (e.g.,

[12] http://www.swift.psu.edu/unassociated/

Table 1
List of Acronyms Used in the Paper

Acronym	Term
1FGL	*Fermi*-Large Area Telescope First Source Catalog
1FGLR	1FGL Refined association catalog
1FHL	First *Fermi*-Large Area Telescope Catalog of Sources Above 10 GeV
1LAC	First Catalog of Active Galactic Nuclei Detected by *Fermi*
1XSPS	Deep Swift X-Ray Telescope Point Source Catalog
2FGL	*Fermi*-Large Area Telescope 2-Year Source Catalog
2FGLR	2FGL Refined association catalog
2LAC	Second Catalog of Active Galactic Nuclei Detected by *Fermi*
2MASS	Two Micron All Sky Survey
3 C	Third Cambridge Catalog of Radio Sources
6dFGS	Six-degree-Field Galaxy Redshift Survey
AGN	Active Galactic Nucleus
AGU	AGN of Uncertain type
AT20G	Australia Telescope 20 GHz Survey
ATNF	Australia Telescope National Facility
BZB	BL Lac object
BZQ	Quasar radio-loud with a flat radio spectrum
CRATES	Combined Radio All-Sky Targeted 8 GHz Survey radio catalog
CSC	*Chandra* Source Catalog
CT	Classification Tree method
FIRST	VLA Faint Images of the Radio Sky at Twenty Centimeters
GB6	Green Bank 6 cm Radio Source Catalog
GLC	Globular Cluster
HMB	High Mass X-ray Binary
KDE	Kernel Density Estimation
IRAF	Image Reduction and Analysis Facility
IRAS	InfraRed Astronomical Satellite
LAT	Large Area Telescope
LBA	Australian Long Baseline Array
LCS1	LBA Calibrator Survey
LORCAT	Low-frequency Radio Catalog of flat-spectrum Sources
LR	Logistic Regression method
MGPS	Molonglo Galactic Plane Survey
MSP	Millisecond Pulsar
NED	NASA/IPAC Extragalactic Database
NOV	Nova
NRAO	National Radio Astronomy Observatory
NVSS	NRAO VLA Sky Survey Catalog
OAGH	Observatorio Astrofisico Guillermo Haro
OAN	Observatorio Astronómico Nacional
PKS	Parkes Southern Radio Source catalog
PMN	Parkes-MIT-NRAO Surveys
PSR	Pulsar
PWN	Pulsar wind nebula
RBSC	*ROSAT* Bright Source Catalog
RFSC	*ROSAT* Faint Source Catalog
SDSS	Sloan Digitized Sky Survey
SED	Spectral Energy Distribution
SFR	Star-forming-H II regions
SNR	Supernova Remnant
SUMSS	Sydney University Molonglo Sky Survey
TEXAS	Texas Survey of Radio Sources at 365 MHz
UGS	Unidentified Gamma-ray Source
VLA	Very Large Array
VLSS	VLA Low-Frequency Sky Survey Discrete Source Catalog
USNO	United States Naval Observatory
XMMSL	*XMM-Newton* Slew Survey
WENSS	Westerbork Northern Sky Survey
WISE	Wide-Field Infrared Survey Explorer
WISH	Westerbork in the Southern Hemisphere Source Catalog
WSRT	Westerbork Synthesis Radio Telescope
WSRTGP	WSRT Galactic Plane Compact 327 MHz Source Catalog

Giommi et al. 2012; López-Caniegoet et al. 2013). Optical spectroscopic campaigns have also been crucial to disentangle and/or confirm the natures of the low-energy counterparts selected with different methods (e.g., Masetti et al. 2013; Shaw et al. 2013a, 2013b; Landoni et al. 2014; Paggi et al. 2014; Massaro et al. 2014b).

The main aim of the analysis presented here is to confirm the current status of the associations for the 1FGL and the 2FGL γ-ray sources. Thus we prepare a single list, created by merging the unique sources in the 1FGL and 2FGL catalogs. On the basis of the information reported in the First *Fermi*-LAT Catalog of Sources Above 10 GeV (1FHL, Ackermann et al. 2013) and in both the First and the Second Catalogs of AGNs Detected by *Fermi* (1LAC and 2LAC, respectively, Abdo et al. 2010b; Ackermann et al. 2011a), together with an extensive literature search in the multifrequency archives, we verify the current status of the γ-ray associations. In addition, we also present new optical spectroscopic observations of eight γ-ray blazar candidates (BCN) selected during our multifrequency study. The result is a refined and merged list of all of the associations for the 1FGL plus 2FGL catalog with updated information on the low-energy counterparts, including specific multifrequency notes.

The paper is organized as follows. In Section 2, we discuss the *Fermi* procedures for assigning identifications and associations with potential counterparts at low energies, and the categories of γ-ray source associations. Section 3 describes the content and main properties of both 1FGL and 2FGL. In Section 4, we introduce an updated γ-ray source classification for the counterparts of the *Fermi*-detected objects. Details on the correlation with multifrequency databases and catalogs are provided in Section 5. In Section 6, we present the refined version of the associations listed in the *Fermi* catalogs (hereafter designated 1FGLR and 2FGLR, respectively). The analysis of the IR colors for the sources associated in 1FGL is provided in Section 7 and new optical spectroscopic observations of γ-ray BCN are presented in Section 8. In Section 9, we compare our results with those achieved from statistical analyses performed on UGSs listed in both 1FGL and 2FGL. In Section 10, we speculate on both the radio–γ-ray and the IR–γ-ray connections for the *Fermi* blazars to check the consistency of sources classified as BCN with these multifrequency behaviors. Our summary and conclusions are provided in Section 11. We use cgs units unless stated otherwise. Spectral indices, α, are defined by flux density, $S_\nu \propto \nu^{-\alpha}$ and WISE magnitudes at [3.4], [4.6], [12], [22] μm (i.e., the nominal bands) are in the Vega system. For numerical results, a flat cosmology was assumed with $H_0 = 67.3\,\mathrm{km\,s^{-1}\,Mpc^{-1}}$, $\Omega_M = 0.315$, and $\Omega_\Lambda = 0.685$ (Planck Collaboration 2014). The astronomical survey and source class acronyms used in the paper are listed in Table 1.

2. CATEGORIES OF γ-RAY SOURCE ASSOCIATIONS

In all of the *Fermi* catalogs, there is an important distinction between *identification* of low-energy counterparts for the *Fermi* sources and *association*. Identification is based on (i) spin or orbital periodicity (e.g., pulsars, binary systems), (ii) correlated variability at other wavelengths (e.g., blazars, active galaxies), or on (iii) the consistency between the measured angular sizes in γ-ray and at lower energies (e.g., supernova remnants, SNRs). On the other hand, the *association* designation indeed depends on the results of different procedures

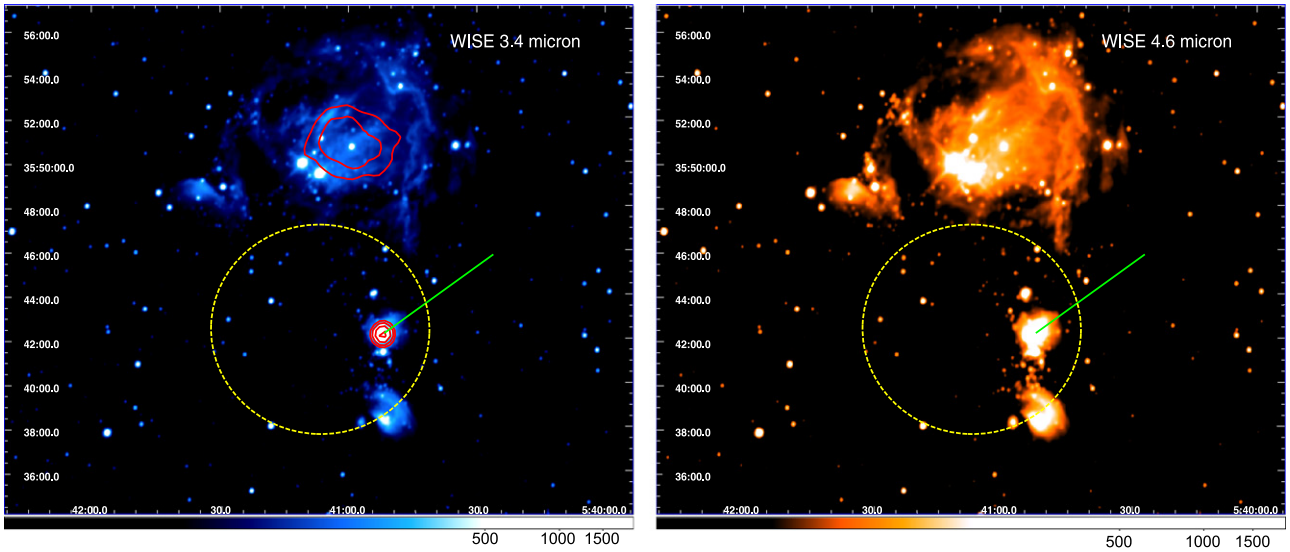

Figure 1. WISE images of the *Fermi* source 1FGLJ0541.1+3542c in two different bands at 3.4 (top) and 4.6 μm (bottom). In each image, the yellow ellipse corresponds to the *Fermi* positional uncertainty region at 68% level of confidence. The red contours on the WISE image at 3.4 μm indicate the radio brightness at 1.4 GHz from NVSS. The radio-infrared extended structure, marked by the green arrow, suggests that a shock occurred in the interstellar medium that could be responsible for the γ-ray emission. The radio source is also detected in the Westerbork Northern Sky Survey (WENSS; Rengelink et al. 1997) and it is associated with an open star cluster.

Table 2
Source Classification For the γ-ray Counterparts

Class	Code
Galactic Sources	
High mass X-ray binary	hmb
Globural cluster	glc
Nova	nov
Millisecond pulsar (MSP)	msp
Pulsar (PSR)	psr
Pulsar wind nebula (PWN)	pwn
Binary star	bin
Star-forming-H II region (SFR)	sfr
(for potential associations with unknown SNRs and/or PWNs and/ or PSRs)	
Supernova remnant (SNR)	snr
Extragalactic Sources	
BL Lac object (BZB)	bzb
Quasar radio loud with flat radio spectrum (BZQ)	bzq
Blazar of uncertain type (BZU)	bzu
Normal galaxy	gal
Radio galaxy	rdg
Starburst galaxy	sbg
Seyfert galaxy	sey
Uncertain Classification	
Blazar candidate	bcn
Unclassified sources	unc
Unidentified γ-ray source	ugs

adopted in both *Fermi* catalogs (Abdo et al. 2010a; Nolan et al. 2012). These procedures are as follow.

1. *The Bayesian association method*: initially applied to associate EGRET sources with flat-spectrum radio sources (e.g., Mattox et al. 1997, 2001; Abdo et al. 2010a), this method assesses the probability of association between a γ-ray source and a candidate counterpart taking into account their local densities. Local density is estimated simply by counting candidates in a nearby region of the sky.
2. *The likelihood ratio method*: used to search for possible counterparts in uniform surveys in the radio and in X-ray bands, this procedure was originally proposed by Richter (1975) and subsequently applied by and modified by de Ruiter et al. (1977), Prestage & Peacock (1983), Wolstencroft et al. (1986), and Sutherland & Saunders (1992).
3. *The log N-log S association method*: this is a modified version of the Bayesian method for blazars taking into account their log N-log S (see Abdo et al. 2010b; Ackermann et al. 2011a, for more details).

There are several differences between the source associations presented between 1FGL and 2FGL mostly related to the γ-ray analysis and to the improvements achieved in the models of Galactic γ-ray diffuse emission as well as in the evaluation of the LAT response functions. Improving the *Fermi* source localization not only makes the search for low-energy counterparts easier but also allows for more accurate estimates of the association probability since they depend on the γ-ray positional uncertainty (see, e.g., Abdo et al. 2010b; Ackermann et al. 2011a). These differences also relate to updates of comparison surveys and catalogs used to search for low-energy counterparts and on multifrequency observations performed on ugs samples.

The use of catalogs/surveys that were previously not considered for the *Fermi* catalog preparation, as for example the IR all-sky survey performed by WISE and the low-frequency radio catalogs, revealing new connections between the low and the high-energy skies (e.g., Massaro et al. 2011a; D'Abrusco et al. 2013; Massaro et al. 2013b) has also decreased the unknown fraction of the γ-ray sky (e.g., Massaro

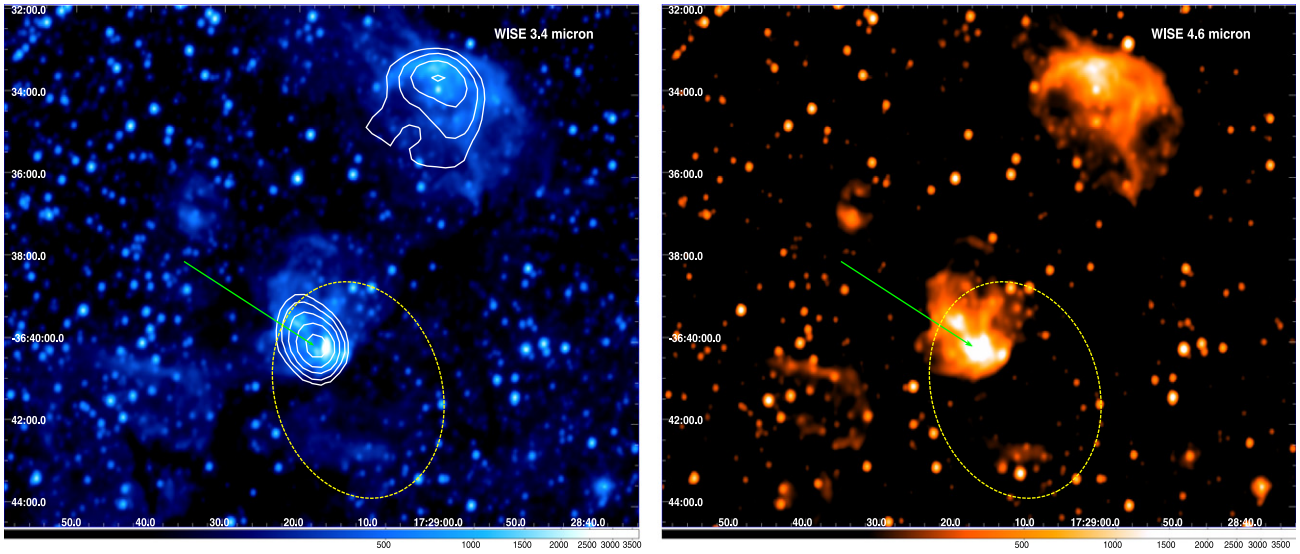

Figure 2. WISE images of the *Fermi* source 1FGLJ1729.1−3641c in two different bands at 3.4 (top) and 4.6 μm (bottom). In each image, the yellow ellipse corresponds to the *Fermi* positional uncertainty region at 68% level of confidence. The white radio contours drawn from the NVSS image are overlaid on the WISE image at 3.4 μm. This is an example of a candidate association with an SFR that includes open star cluster 165 from the Northern and Equatorial Milky Way catalog built with 2MASS observations (Bica et al. 2003).

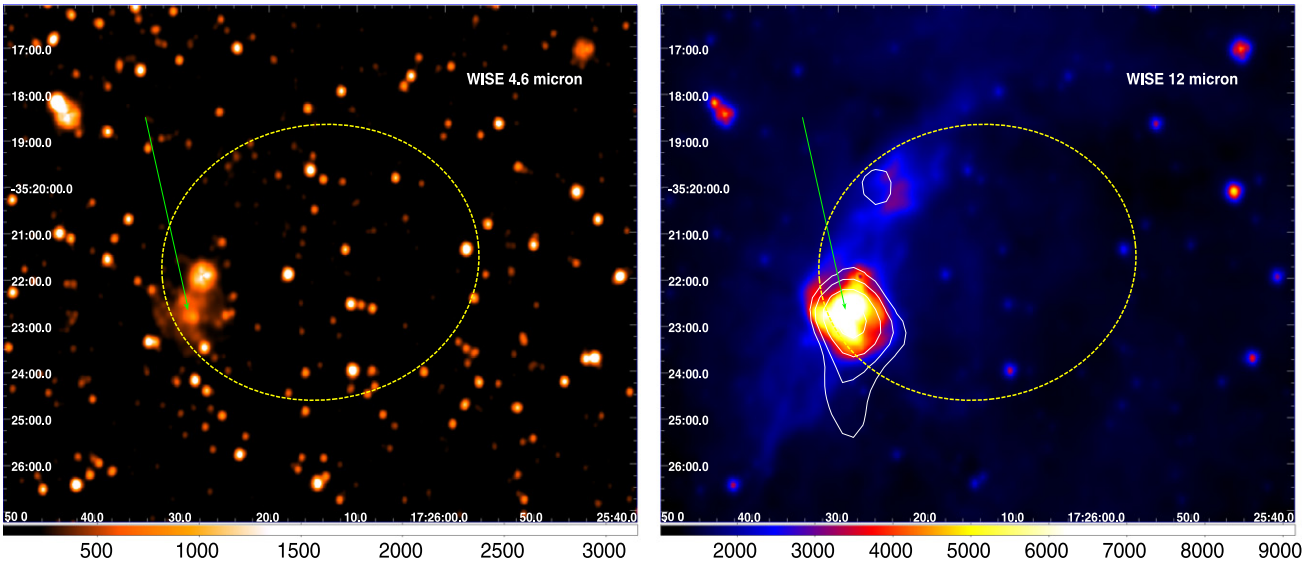

Figure 3. WISE images of the *Fermi* source 1FGLJ1726.2−3521c in two different bands at 4.6 (top) and 12 μm (bottom). In each image, the yellow ellipse corresponds to the *Fermi* positional uncertainty region at 68% level of confidence. The white contours overlaid on the WISE image at 12 μm are the 1.4 GHz radio emission from NVSS. The radio-infrared extended structure, marked by the green arrow, clearly indicates that a shock occurred in the interstellar medium within the *Fermi* positional uncertainty region. This could be responsible for the γ-ray emission.

et al. 2012b, 2013a). This affects the *Fermi* associations because the methods adopted to assign low-energy counterparts depend on the source densities of the catalogs (Ackermann et al. 2011a; Nolan et al. 2012). A better estimate of the counterpart density leads to a better estimate of the false positive associations and of the association probability and this implies that a previously unassociated source could have an assigned counterpart in a new release of the *Fermi* catalog.

Motivated by the changes occurring between the 1FGL and the 2FGL associations, here we propose to introduce, together with identified and associated sources, the category of *"candidate associations."* These are γ-ray sources that have a potential low-energy counterpart in a specific class of well-known γ-ray emitters lying within the *Fermi* positional uncertainty region at a 95% level of confidence and/or having angular separations between the *Fermi* and counterpart positions smaller than the maximum for all of the associated sources of the same class. Candidate associations have the potential to be promoted to associations in the future (see Section 4).

We considered only a few kinds of sources as counterpart classes for the candidate associations: (i) blazar-like sources, as defined in the following, (ii) known pulsars (PSRs), (iii) pulsar wind nebulae (PWNs), SNRs, and star-forming and H II regions (hereinafter simply indicated as SFRs). The first two source classes constitute the two largest populations of known γ-ray emitters while the other choices were considered because 15 out of the 44 SNRs and 10 out of the 63 PSRs and PWNs

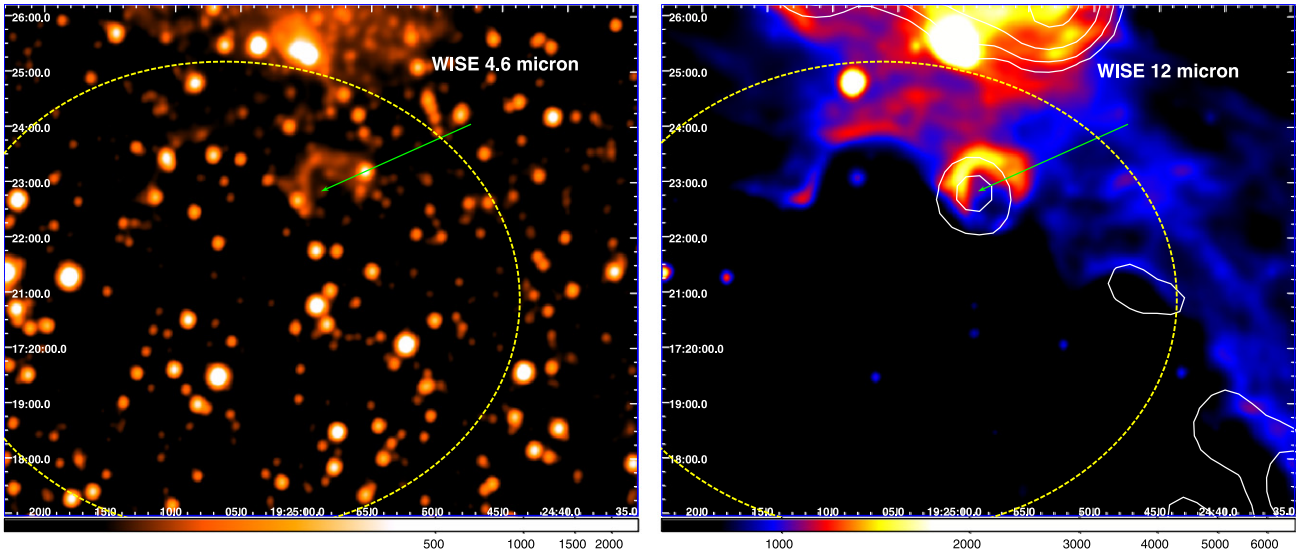

Figure 4. WISE images of the *Fermi* source 1FGLJ1925.0+1720c in two different bands at 4.6 (top) and 12 μm (bottom). In each image, the yellow ellipse corresponds to the *Fermi* positional uncertainty region at 68% level of confidence. The white contours overlaid on the WISE image at 12 μm are the 1.4 GHz radio emission from NVSS. The ring-shaped structure, indicated by the green arrow, is extended for about 87″ and resembles an unknown SNR or PWN. It clearly lies within the *Fermi* positional uncertainty region and is also emitting in the radio band. This is a clear example of a candidate association with an SFR including a potential SNR/PWN for which additional multifrequency observations are necessary to confirm its origin.

Table 3
Multifrequency Notes for Pulsars

Symbol	Comment
b	PSR in a binary system
e	PSR detected in γ rays by the Compton γ-ray Observatory
g	PSR discovered in LAT γ-ray data
m	MSP
p	Pulsar discovered by the Pulsar Search Consortium (PSC)
r	PSR discovered in the radio
u	PSR discovered using a *Fermi*-LAT seed position
x	PSR discovered in X-rays

associated in 1FGL lie within SFRs and a similar situation occurs for 2FGL.

Our choice concerning SFRs, especially for the most massive cases, is indeed motivated by the possibility that they could host type O and/or B stars, potentially associated with open star clusters, which are relatively likely to have some members that have progressed to become a PSR, PWN, and/or SNR, that are well known classes of γ-ray sources (see also Montmerle 1979, 2009).

In addition, considering SFRs as candidate associations is also motivated by the recent idea, partially supported by the *Fermi* discovery of γ-ray emission arising from Eta Carinae (Abdo et al. 2010c), that shells detected in the radio, IR, and X-ray could mark the termination shocks of stellar winds. These winds interacting with the stars' natal molecular clouds can be considered as plausible sites for the acceleration of particles that emit γ-rays (e.g., Araudo et al. 2007; Bosch-Ramon et al. 2010; Rowell et al. 2010). Bowshocks are associated with many source classes such as PSRs, cataclysmic variables, colliding wind binaries, cometary H II regions, and particles accelerated therein can radiate up to the MeV–GeV energy range (see e.g., Del Valle & Romero 2012). However, we remark that evidence of γ-ray emission from colliding wind binaries associated with Wolf–Rayet stars was not found by *Fermi* for a select sample of seven sources (Werner et al. 2013), although, as highlighted by the same authors, searching for such γ-ray detections is extremely complicated due to the uncertainties of the diffuse emission in the Galactic plane.

Some candidate associations lack multifrequency information as well as correct spectroscopic identifications but *exhibit some characteristic* features, typical of known γ-ray emitters, mainly blazars and PSRs. They were not associated in the previous releases of the *Fermi* catalogs, mostly because they were not listed in one of the appropriate comparison catalogs of potential counterparts used to associated *Fermi* sources. However, once follow up observations *were* performed (see, e.g., Masetti et al. 2013; Paggi et al. 2013; Petrov et al. 2013; Landoni et al. 2014; Massaro et al. 2014b, for blazar-like candidates), they could be promoted to associated sources in new releases of the *Fermi* catalogs. In addition, within this category we also considered *Fermi* sources that have SFRs within their γ-ray positional uncertainty regions for which multifrequency observations could reveal the presence of unknown PSRs, PWNs and SNRs, already counterparts of $\sim$5% of the γ-ray sources.

We emphasize three advantages obtained from introducing the concept of candidate associations.

1. Designating a candidate association category allows us to flag potential counterparts that might be associated or identified in future releases of the *Fermi* catalogs, as previously occurred for 171 1FGL recognized sources, classified and associated in 2FGL. This also facilitates planning follow up multifrequency observations, in particular, spectroscopic observations, necessary to determine and/or confirm their nature.
2. The category of candidate associations permits us to establish the number of *Fermi* sources not yet having potential counterparts. Precise knowledge of this number is extremely relevant for setting better constraints on dark matter scenarios (e.g., Mirabal et al. 2012; Zechlin et al. 2012; Mirabal 2013a, 2013b; Berlin & Hooper 2014).

Table 4
Refined Associations of the *Fermi* Catalogs (First 30 Lines)

1FGL Name	2FGL Name	1FHL Name	Category	Counterpart1	Notes1	z	Inside	Include	Class (ctp1)	R.A. (ctp1) (J2000)	Decl. (ctp1) (J2000)	B (ctp1) (mag)	R (ctp1) (mag)	Counterpart2	Notes2	Class (ctp2)	R.A. (ctp2) (J2000)	Decl. (ctp2) (J2000)	B (ctp2) (mag)	R (ctp2) (mag)	$\pi_{\mathrm{KDE,\,BZB}}$	$\pi_{\mathrm{KDE,\,BZQ}}$
Col. 1	Col. 2	Col. 3	Col. 4	Col. 5	Col. 6	Col. 7	Col. 8	Col. 9	Col. 10	Col. 11	Col. 12	Col. 13	Col. 14	Col. 15	Col. 16	Col. 17	Col. 18	Col. 19	Col. 20	Col. 21	Col. 22	Col. 23
1FGL J0000.8+6600c			U						ugs													
1FGL J0000.9−0745	2FGL J0000.9−0748		A	BZBJ0001−0746		0.0			bcn	00:01:18.01	−07:46:26.90	18.14	17.19								84.2	22.5
1FGL J0001.9−4158	2FGL J0001.7−4159		C	1RXS J000135.5−415519	w,M,U,X				unc	00:01:35.50	−41:55:18.98	20.53	19.08	SUMSS J000133−415524	S,M,x — SED in Takeuchi +13	unc	00:01:33.05	−41:55:24.31	18.95	18.01	0.3	0.0
1FGL J0003.1+6227	2FGL J0002.7+6220		C	NVSS J000225+622937	N,M,U				unc	00:02:25.24	+62:29:37.10	17.63	20.17									
1FGL J0004.3+2207	2FGL J0004.2+2208		U						ugs													
1FGL J0004.7−4737	2FGL J0004.7−4736		A	BZQJ0004−4736		0.88			bzq	00:04:35.68	−47:36:18.61											
1FGL J0005.1+6829	2FGL J0007.7+6825c		C	WISE J000345.96+681640.9	w				unc	00:03:45.96	+68:16:40.91	17.63	15.63								75.1	0.3
1FGL J0005.7+3815	2FGL J0006.1+3821		A	BZQJ0005+3820		0.229			bzq	00:05:57.18	+38:20:15.11											
1FGL J0006.9+4652			U						ugs													
1FGL J0007.0+7303	2FGL J0007.0+7303	1FHL J0007.3+7303	I	PSR J0007+7303	g		GBH41.83992+0.02242 and G110.21+2.63	SNR G119.5+10.2	psr in snr	00:06:34.20	+73:11:06.60											
1FGL J0008.3+1452			U						ugs													
1FGL J0008.9+0635	2FGL J0009.0+0632		A	BZBJ0009+0628	V,T,N,87,w,M,s,U,g,c,rf–> (z=? - BL Lac — Ahn+12, Massaro+14)	0.0			bcn	00:09:03.93	+06:28:21.24	19.06	18.42								64.9	21.3
1FGL J0009.1+5031	2FGL J0009.1+5030	1FHL J0009.2+5032	A	NVSS J000922+503028	L,N,U,x –SED in Takeuchi +13–> (z = ? - *BL Lac* –Shaw+13)	0.0			bcn	00:09:22.53	+50:30:28.91	19.74	19.35								45.5	0.0
1FGL J0011.1+0050	2FGL J0011.3+0054		A	BZQJ0011+0057		1.492			bzq	00:11:30.40	+00:57:51.80											
1FGL J0013.1−3952	2FGL J0012.9−3954		A	BZBJ0012−3954		0.0			bcn	00:12:59.91	−39:54:26.10	18.14	18.05								63.1	74.3
1FGL J0013.7−5022			A	BZBJ0014−5022		0.0			bcn	00:14:11.22	−50:22:32.59	19.36	18.82								13.1	0.2
1FGL J0016.6+1706			U						ugs													

Table 4
(Continued)

1FGL Name	2FGL Name	1FHL Name	Category	Counterpart1	Notes1	z	Inside	Include	Class (ctp1)	R.A. (ctp1) (J2000)	Decl. (ctp1) (J2000)	B (ctp1) (mag)	R (ctp1) (mag)	Counterpart2	Notes2	Class (ctp2)	R.A. (ctp2) (J2000)	Decl. (ctp2) (J2000)	B (ctp2) (mag)	R (ctp2) (mag)	$\pi_{KDE,BZB}$	$\pi_{KDE,BZQ}$
Col. 1	Col. 2	Col. 3	Col. 4	Col. 5	Col. 6	Col. 7	Col. 8	Col. 9	Col. 10	Col. 11	Col. 12	Col. 13	Col. 14	Col. 15	Col. 16	Col. 17	Col. 18	Col. 19	Col. 20	Col. 21	Col. 22	Col. 23
1FGL J0017.4−0510	2FGL J0017.6−0510		A	BZQJ0017−0512		0.227			bzq	00:17:35.82	−05:12:41.69											
1FGL J0017.7−0019	2FGL J0017.4−0018		A	BZQJ0016−0015		1.577			bzq	00:16:11.09	−00:15:12.38											
1FGL J0018.6+2945	2FGL J0018.5+2945	1FHL J0018.6+2946	A	BZBJ0018+2947		0.1			bzb	00:18:27.75	+29:47:30.41											
1FGL J0019.3+2017			A	BZBJ0019+2021		0.0			bzb	00:19:37.85	+20:21:45.61											
1FGL J0021.7−2556	2FGL J0021.6−2551		A	BZBJ0021−2550		0.0			bcn	00:21:32.50	−25:50:49.20	16.86	17.51								93.3	2.4
1FGL J0022.2−1850	2FGL J0022.2−1853	1FHL J0022.2−1853	A	NVSS J002209−185332	N,6,U,g,X–> (z=? − BL Lac −Shaw+13)	0.0			bcn	00:22:09.16	−18:53:32.78	18.07	16.95								99.4	3.6
1FGL J0022.5+0607	2FGL J0022.5+0607	1FHL J0022.5+0607	A	BZBJ0022+0608		0.0			bzb	00:22:32.44	+06:08:04.31											
1FGL J0023.0+4453	2FGL J0023.2+4454		A	BZQJ0023+4456		1.062			bzq	00:23:35.44	+44:56:35.81											
1FGL J0023.5+0930	2FGL J0023.5+0924		A	PSR J0023+0923	mbrup				msp	00:23:16.89	+09:23:24.18											
1FGL J0023.9−7204	2FGL J0023.9−7204		A	GCl 1 (47 Tuc)					glc	00:24:05.36	−72:04:53.20											
1FGL J0024.6+0346	2FGL J0024.5+0346		A	BZQJ0024+0349		0.545			bzq	00:24:45.21	+03:49:03.50											
1FGL J0028.9−7028			U						ugs													
1FGL J0029.9−4221	2FGL J0030.2−4223		A	BZQJ0030−4224		0.495			bzq	00:30:17.58	−42:24:46.01											

Notes. Column description. (1): 1FGL name, (2): 2FGL name, (3): 1FHL name, (4): γ-ray source category (I—identified; A—associated; C—candidate; U—unidentified; see Section 2 for details), (5): name of the first low-energy counterpart, (6): multifrequency notes on the first low-energy counterpart, (7): redshift estimate if the source is extragalactic (in the online version of the catalog there is also a note if the z measurement is uncertain), (8): notes if the first low-energy counterpart lies inside a SFR/SNR/PWN, (9): notes if the first low-energy counterpart includes a PSR/MSP, (10): source class for the first low-energy counterpart (see Section 4 for details), (11): R.A. (J2000) for the first low-energy counterpart, (12): decl. (J2000) for the first low-energy counterpart, (13): B magnitude for the first low-energy counterpart taken from the USNO-B1 Catalog (Monet et al. 2003), only for the BCN and the unc sources, (14): R magnitude for the first low-energy counterpart taken from the USNO-B1 Catalog (Monet et al. 2003), only for the BCN and the unc sources, (15): name of the second low-energy counterpart, (16): multifrequency notes on the second low-energy counterpart, (17): source class for the second low-energy counterpart (see Section 4 for details), (18): R.A. (J2000) for the second low-energy counterpart, (19): decl. (J2000) for the second low-energy counterpart, (20): B magnitude for the second low-energy counterpart taken from the USNO-B1 Catalog (Monet et al. 2003), only for the BCN and the unc sources, (21): R magnitude for the second low-energy counterpart taken from the USNO-B1 Catalog (Monet et al. 2003), only for the BCN and the unc sources, (22): probability that the first low-energy counterpart has infrared colors similar to the known 1FGL BZBs estimated with the KDE method (see Section 7 for details), (23): probability that the first low-energy counterpart has infrared colors similar to the known 1FGL BZQs estimated with the KDE method (see Section 7 for details). Symbols used for the multifrequency notes are all reported in Section 5 together with the references of the

catalogs/surveys. References for the optical spectra reported in the table: Ackermann et al. (2011a), Ahn et al. (2012), Baker et al. (1995), Bauer et al. (2000), Bade et al. (1995), Beuermann et al. (1999), Bikmaev et al. (2008), Britzen et al. (2007), Drinkwater et al. (1997), Healey et al. (2008), Hewett & Wild (2010), Hewitt & Burbidge (1989), Johnston et al. (1995), Jones et al. (2004), Jones et al. (2009), Landoni et al. (2014) Landt et al. (2001), Lister et al. (2011), Mao (2011), Maza et al. (1995), Marti et al. (2004), Masetti et al. (2013), Massaro et al. (2014c) Mitton et al. (1977), Paggi et al. (2013), Quintana & Ramirez (1995), Schwope et al. (2000), Shaw et al. (2013a, 2013b), Stern & Assef (2013), Stickel & Kuehr (1996a, 1996b) Titov et al. (2011) , Vandenbroucke et al. (2010), Vettolani et al. (1989), Takeuchi et al. (2013), Thompson et al. (1990), Tsarevsky et al. (2005), White et al. (1988).

(This table is available in its entirety in machine-readable forms.)

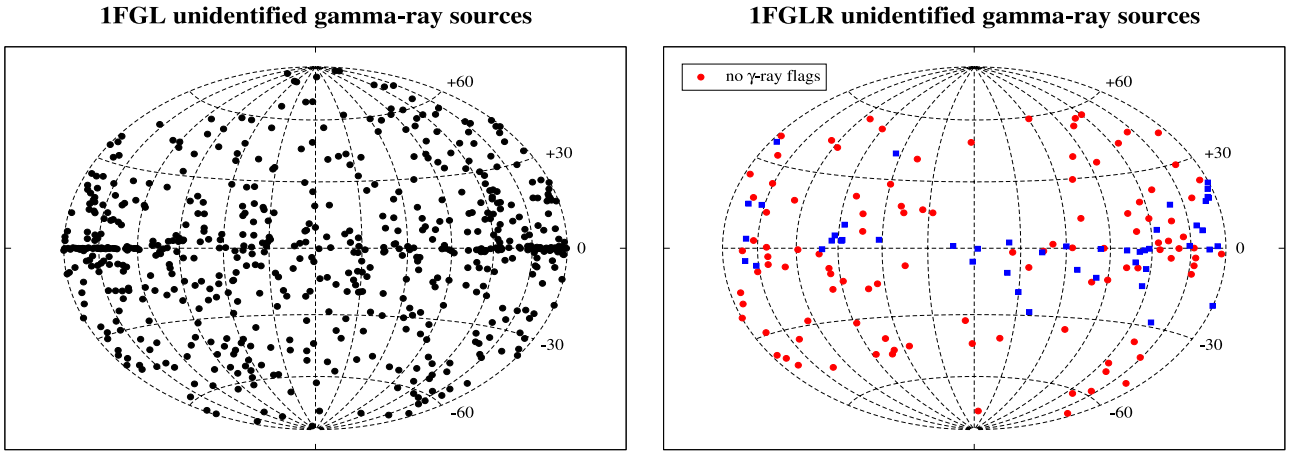

Figure 5. All-sky distribution of UGSs in 1FGL (left) compared with those listed in 1FGLR (right panel). *Red circles mark those UGSs with no γ-ray analysis flags and blue squares those with a flag.* The projection is the Hammer–Aitoff projection in Galactic coordinates

Table 5
Summary of Categories for the γ-ray Source Associations in the Refined Association List of Both *Fermi* Catalogs

	1FGLR				2FGLR			
Class	ID.	Ass.	Cac.	Tot.	ID.	Ass.	Can.	Tot.
Galactic								
bin	0	1	0	1	0	1	0	1
hmb	3	0	1	4	4	0	0	4
glc	0	9	0	9	0	11	0	11
nov	0	0	0	0	1	0	0	1
msp	26	16	8	50	26	17	8	51
psr	53	8	31	92	56	12	30	98
pwn	0	8	2	10	2	6	1	9
snr	3	38	5	46	6	55	5	66
sfr	0	0	54	54	0	0	63	63
Extragalactic								
bzb	7	231	1	239	7	270	0	277
bzq	15	271	1	287	18	320	0	338
bzu	2	46	0	48	2	52	0	54
gal	1	5	0	6	2	4	0	6
rdg	0	5	0	5	1	7	0	8
sbg	0	3	0	3	0	3	0	3
sey	0	2	0	2	0	3	0	3
Uncertain								
bcn	0	188	25	213	0	242	29	271
unc	1	49	178	228	1	173	146	320
ugs	0	0	0	154	0	0	0	289

Note. Col. (1) Source class. Col. (2) ID.—identified. Col. (3) Ass.—associated. Col. (4) Can.—candidate associations.

3. For all of the methods adopted to associate sources in the *Fermi* catalogs, the resulting associations depend on the comparison catalog/survey used. The same low-energy counterpart may be associated with a *Fermi* source using a certain catalog but not in a different survey, even when the positions in the two catalogs are the same. This occurs because the source density of the comparison catalogs, which is used to determine the probability of false positive associations, affects the association probability. Thus, observing these candidate associations with follow up campaigns to determine their natures will permit us to add blazars and PSRs to the correct comparison catalogs and associate them in future releases of the *Fermi* surveys.

To reiterate the importance of having candidate associations, we highlight the recent work of Schinzel et al. (2014) on radio very long baseline interferometry observations of *Fermi* unassociated sources in 2FGL (see also Petrov et al. 2013). In the final list of high-confidence associations presented in Schinzel et al. (2014), more than 90% of the sources are also detected in major radio surveys such as the National Radio Astronomy Observatory (NRAO) Very Large

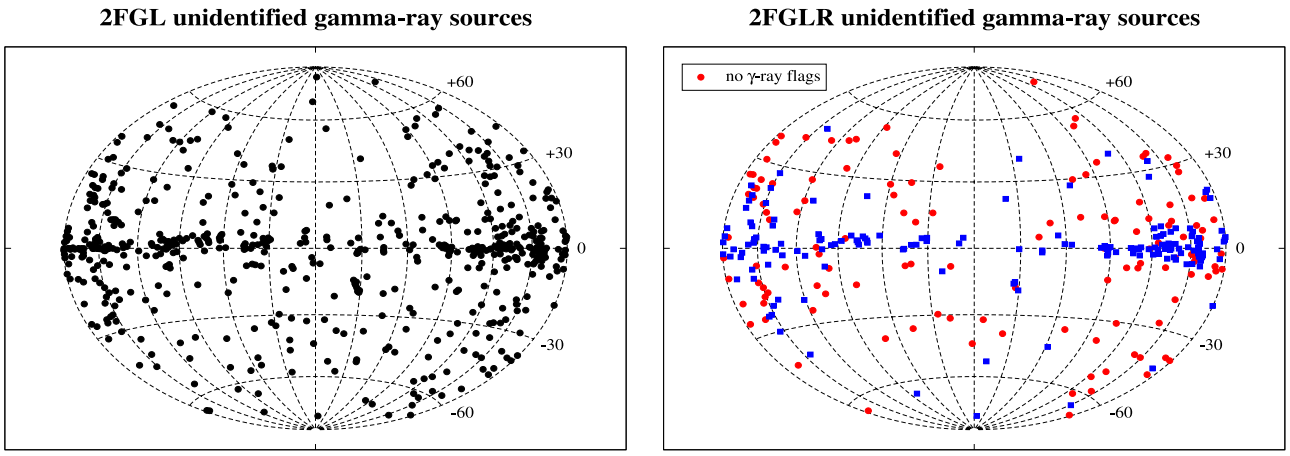

Figure 6. All-sky distribution of UGSs in 2FGL (left) compared with those listed in 2FGLR (right panel). Red circles mark those UGSs with no γ-ray analysis flags and blue squares those with a flag.

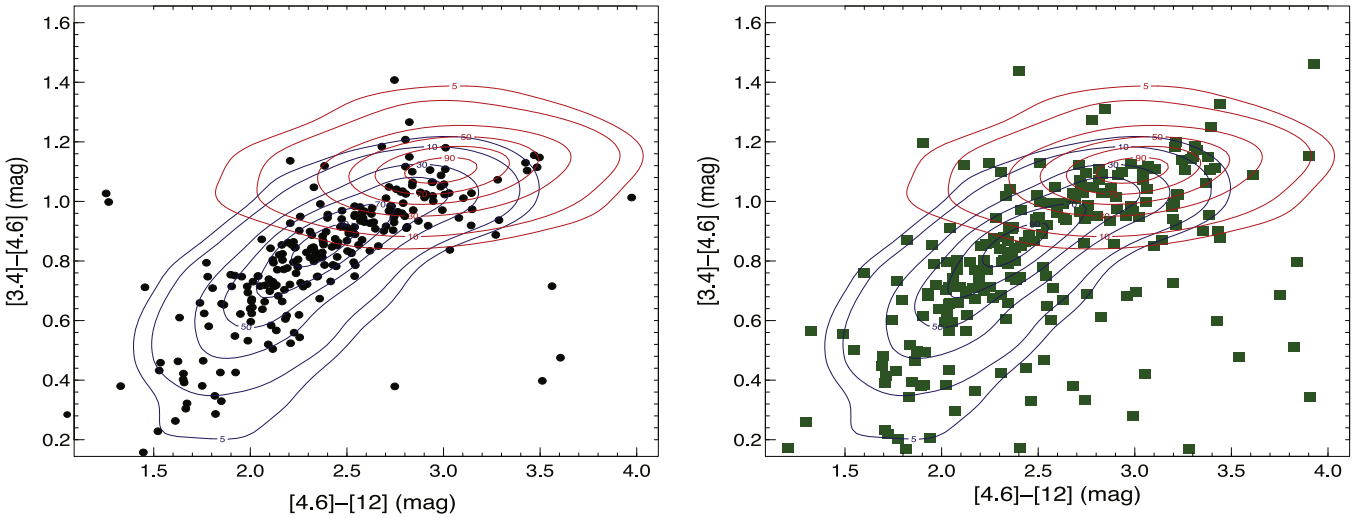

Figure 7. Isodensity contours drawn from the KDE technique for the *Fermi*-Roma-BZCAT blazars (i.e., training sample) that constitute the WISE γ-ray Strip (Massaro et al. 2011a) in the [3.4]-[4.6]-[12] μm color–color plot. Blue contours were computed from the infrared colors of the BZBs while the red ones were derived from the BZQs. The infrared colors of the sources classified as BCN (top—black circles) and unc (bottom—green squares) are also reported to show their consistency with the WISE γ-ray Strip. The numbers appearing close to each contour correspond to the values of $\pi_{\rm KDE}$ in both panels. The last contour correspond to 95% confidence level (see Section 7 for details). A similar analysis for the active galaxies of uncertain type listed in 2FGL was already performed in Massaro et al. (2012a). Here this study has been repeated for both 1FGLR and 2FGLR, and the refined association list of the *Fermi* catalogs.

Table 6
Log and Results of Optical Spectroscopic Observations

Fermi Name	Obs. Date yyyy-mm-dd	Exposure (sec)	Class	z	Spectral Features
1FGL J1548.7+6311	2014 Jun 28	2x1800	BL Lac	0.269	Ca II H&K, G, Hβ, Mg I
1FGL J1844.1+1547	2014 Jun 29	2x1800	BL Lac	?	none
1FGL J2014.4+0647	2014 Jun 29	2x1800	BL Lac	0.341	Ca II H&K, G, Hβ, Mg I
1FGL J2133.4+2532	2014 Jun 29	2x1800	BL Lac	0.294	Ca II H&K, G, Hβ, Mg I
2FGL J1848.6+3241	2014 Jul 02	2x1800	QSO	0.981	Mg II, [O II] λ3727
2FGL J2021.5+0632	2014 Jul 02	1800	QSO	0.217	Hγ, Hβ, [O III] λ4959 & λ5007
2FGL J2031.0+1938	2014 Jul 01	2x1800	BL Lac	0.668?	Mg II?
2FGL J1719.3+1744	2014 Jun 30	2x1800	BL Lac	?	none
2FGL J1801.7+4405	2014 Jun 30	2x1800	QSO	0.663	Mg II, [O II] λ3727
1FGL J1942.7+1033	2014 Jun 29	2x1800	BL Lac	?	none
1FGL J2300.4+3138	2014 Jul 01	2x1800	BL Lac	?	unid. abs. systems
1FGL J2341.6+8015	2014 Aug 28	3x1800	BL Lac	?	none

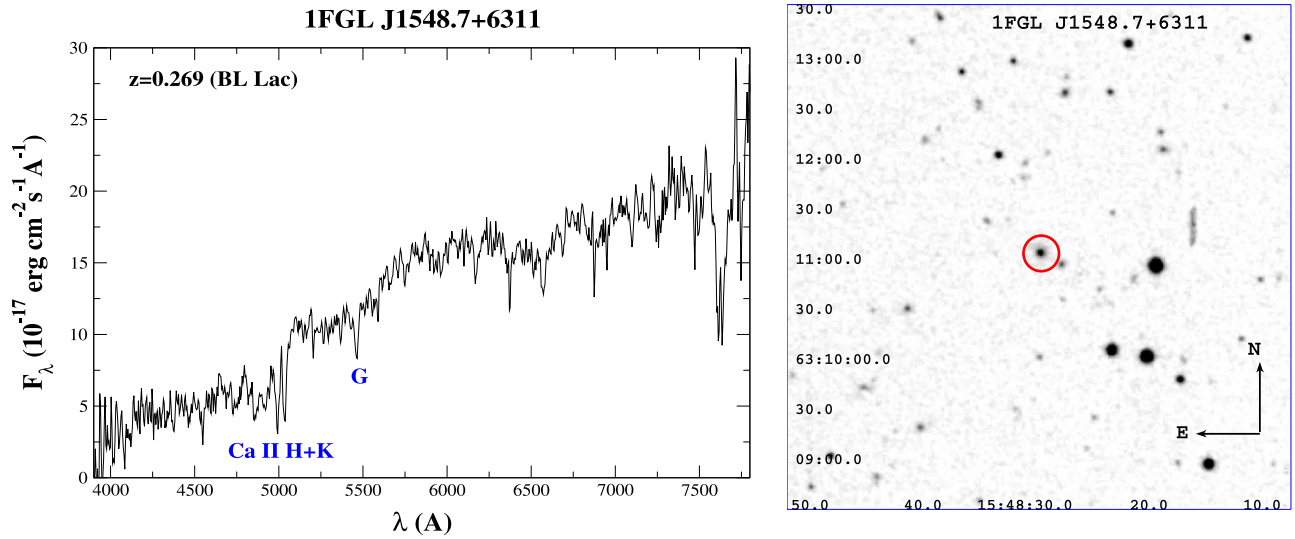

Figure 8. (Upper panel) Optical spectra of the counterpart associated with 1FGL J1548.7+6311 observed at OAN in San Pedro Mártir (México) on 2014 June 28. The absorption features identified as Ca II H&K and the G band used to determine its redshift are marked. The source has been classified as a BL Lac. (Lower panel) 5′ × 5′ finding chart from the Digitized Sky Survey (red filter). The potential counterpart of 1FGL J1548.7+6311, the target of our observation, is indicated by the red circle.

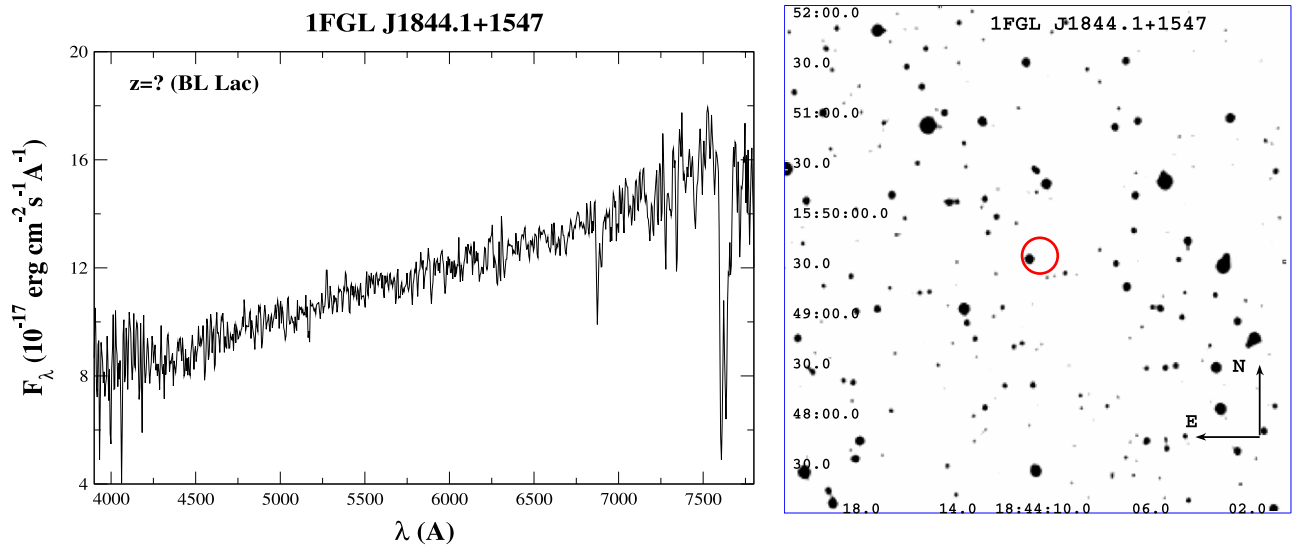

Figure 9. (Upper panel) Optical spectra of the counterpart associated with 1FGL J1844.1+1547 observed at OAN in San Pedro Mártir (México) on 2014 June 29. The source has been classified as a BL Lac on the basis of its featureless continuum. (Lower panel) 5′ × 5′ finding chart from the Digitized Sky Survey (red filter). The potential counterpart of 1FGL J1844.1+1547, the target of our observation, is indicated by the red circle.

Array (VLA) Sky Survey Catalog (NVSS; Condon et al. 1998) and the Sydney University Molonglo Sky Survey (SUMSS; Mauch et al. 2003). These counterparts were not associated using the methods adopted in the *Fermi* catalogs due to the high density of sources at low flux levels in the above surveys. However, thanks to the high-resolution radio follow up observations, which revealed the presence of radio compact cores, it has been possible to use a different selected sample of potential counterparts to find new associations via the likelihood procedure (Petrov et al. 2013; Schinzel et al. 2014). Thus it is extremely important to have targets for follow up observations which, once performed, will allow us to insert the potential counterparts into the correct catalogs used to search γ-ray associations.

Identifications, associations, and candidate associations' of γ-ray sources are labeled in both refined versions of the *Fermi* catalogs as the *category of the γ-ray source association*. These are defined as *identified* (I), *associated* (A), *and candidate association* (C) in the tables, while sources for which no potential counterpart was found are assigned to the ugs category (U).

3. THE *FERMI* CATALOGS

3.1. The Fermi-LAT First Source Catalog

The 1FGL catalog[13] contains 1451 sources detected and characterized in the 100 MeV–100 GeV energy range. For each *Fermi* source listed therein, positional uncertainty regions at 68 and 95% confidence levels resulting from spectral fits as well as flux measurements in five energy bands are reported (Abdo

[13] http://fermi.gsfc.nasa.gov/ssc/data/access/lat/1yr_catalog/

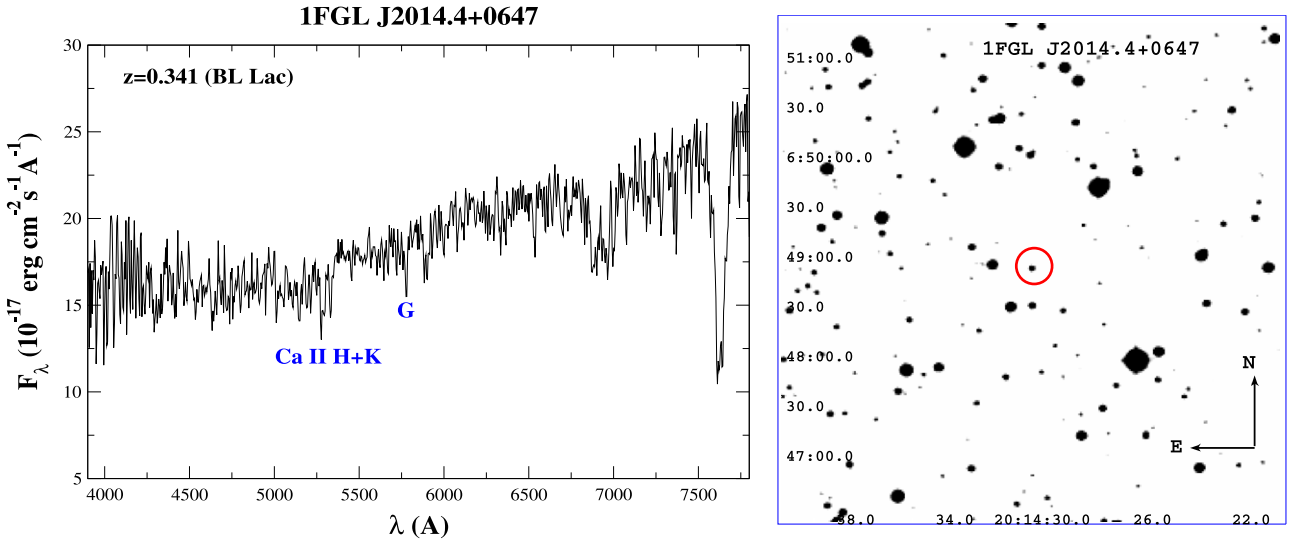

Figure 10. (Upper panel) Optical spectra of the counterpart associated with 1FGL J2014.4+0647 observed at OAN in San Pedro Mártir (México). The source was observed twice on 2014 June 29 and on 2014 June 30 and both spectra are shown. The absorption features identified as Ca II H&K and the G band used to determine its redshift are marked. The source has been classified as a BL Lac. (Lower panel) 5′ × 5′ finding chart from the Digitized Sky Survey (red filter). The potential counterpart of 1FGL J2014.4+0647 is indicated by the red circle.

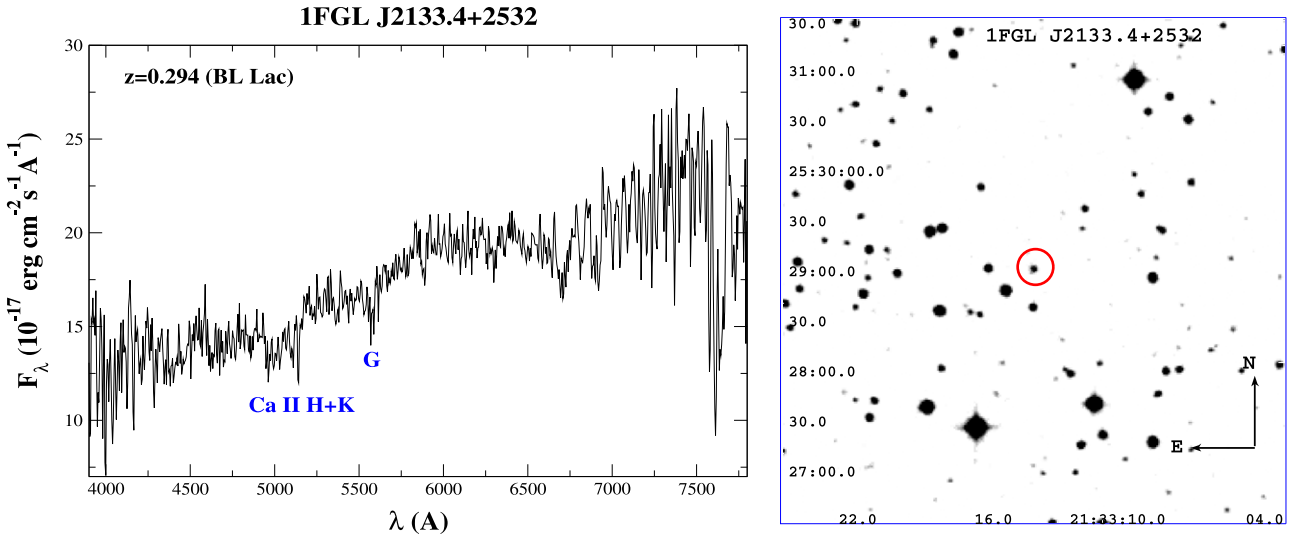

Figure 11. (Upper panel) Optical spectra of the counterpart associated with 1FGL J2133.4+2532 observed at OAN in San Pedro Mártir (México) on 2014 June 29. The absorption features identified as Ca II H&K and the G band used to determine its redshift are marked. The source has been classified as a BL Lac. (Lower panel) 5′ × 5′ finding chart from the Digitized Sky Survey (red filter). The potential counterpart of 1FGL J2133.4+2532 is indicated by the red circle.

et al. 2010a). Firm identification or plausible association with a low-energy counterpart were provided for each 1FGL source on the basis of comparison with other astronomical catalogs and on the association procedures previously mentioned (see Section 2 and Abdo et al. 2010a for details).

The published 1FGL catalog lists several classes of counterparts: 63 PSRs, 7 associated plus 56 identified (24 of them discovered thanks to *Fermi*-LAT observations); 2 PWNs; 44 γ-ray sources corresponding to 38 SNRs, 41 associated and 3 identified; 8 globular clusters (GLCs); 2 high-mass X-ray binaries (HMB), all identified; 295 BL Lac objects (BZBs); 278 flat spectrum radio quasars (BZQs); 28 non-blazar-like AGNs; 92 AGNs of uncertain type (AGUs); 6 normal galaxies; and 2 starburst galaxies. The remaining 630 *Fermi* sources are all UGSs.

A detailed comparison between the 1FGL and the 2FGL catalogs is reported in Nolan et al. (2012). There are 1099 sources included in both *Fermi* catalogs with only 381 1FGL sources being listed in the 1FHL (Ackermann et al. 2013). It is worth noting that 267 out of 1099 sources in common between 1FGL and 2FGL changed classification from 1FGL to 2FGL, and among them 172 previously unassociated in 1FGL obtained an assigned low-energy counterpart in 2FGL. This sample of modified associations includes 16 sources indicated as generic AGNs that have been classified plus 1 that became a ugs; 54 AGUs that have been recognized as blazars (either BZBs or BZQs) and 2 as AGNs; and then 17 blazars actually changed their classification from 1FGL to 2FGL thanks to new spectroscopic data available and, among them, six actually disappeared since they were listed in the 2FGL as unassociated,

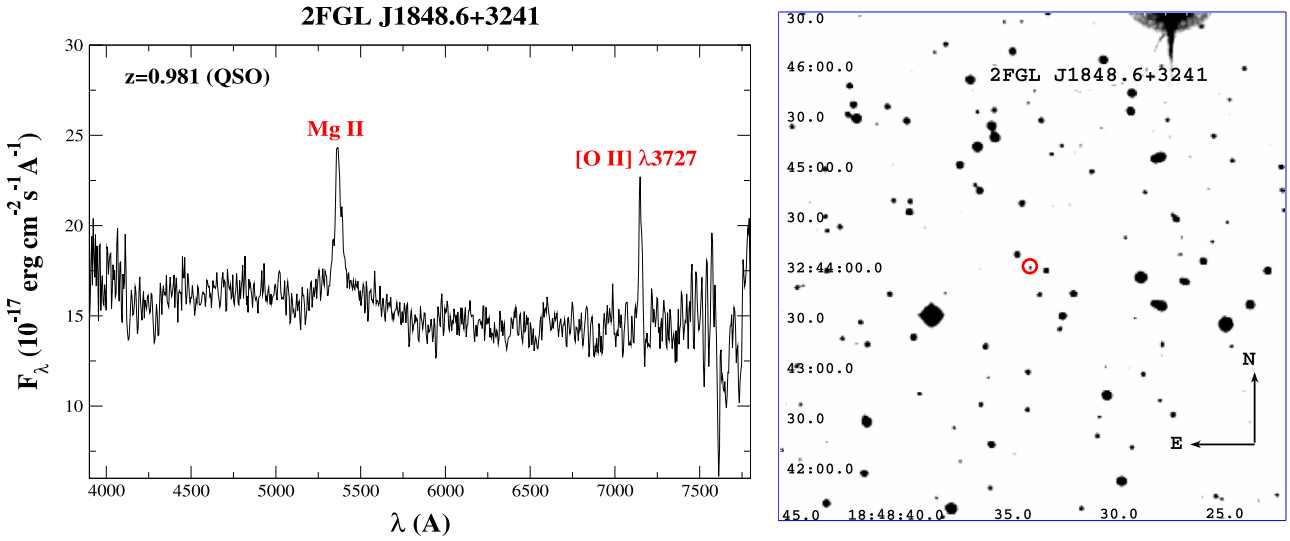

Figure 12. (Upper panel) Optical spectra of the counterparts associated with 2FGL J1848.6+3241 observed at OAN in San Pedro Mártir (México) on 2014 July 2. The emission lines marked allowed us to estimate their redshift. The source has been classified as a QSO. (Lower panel) $5' \times 5'$ finding chart from the Digitized Sky Survey (red filter). The potential counterpart of 2FGL J1848.6+3241 is indicated by the red circle.

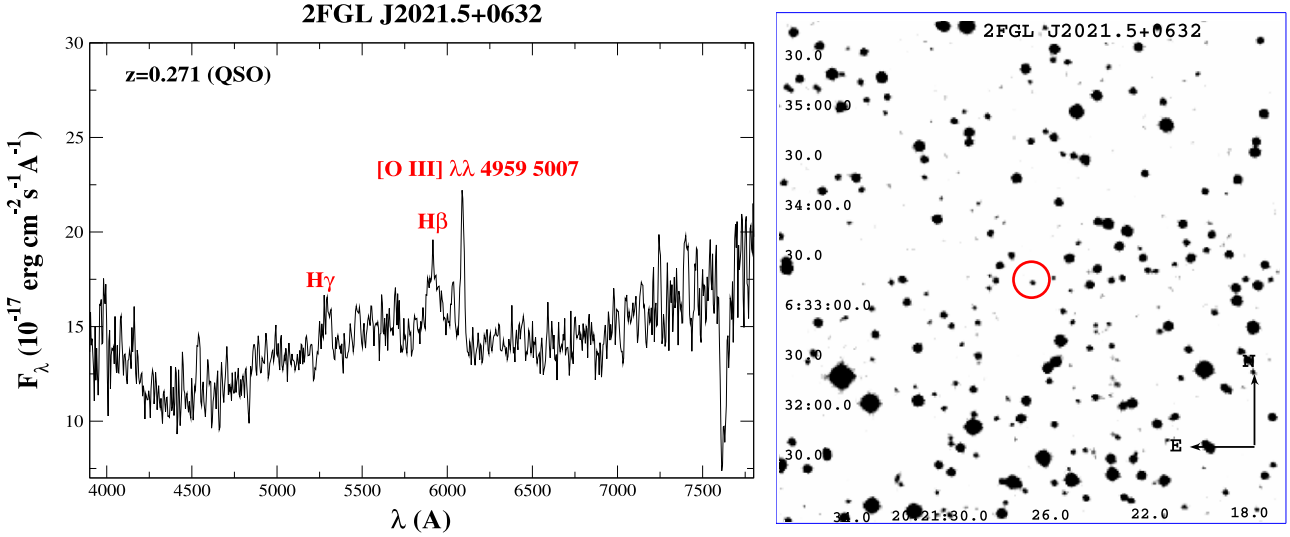

Figure 13. (Upper panel) Optical spectra of the counterparts associated with 2FGL J2021.5+0632 observed at OAN in San Pedro Mártir (México) on 2014 July 2. The emission lines marked allowed us to estimate their redshift. The source has been classified as a QSO. (Lower panel) $5' \times 5'$ finding chart from the Digitized Sky Survey (red filter). The potential counterpart of 2FGL J2021.5+0632 is indicated by the red circle.

as occurred for five other sources of Galactic origin (i.e., PSRs, PWNs, and SNRs). On the other hand, there are 172 UGSs of 1FGL that appear to be associated in 2FGL: 20 associated with PSRs, 11 with SNRs, and 1 with a GLC, while all of the others are associated with various AGN classes (i.e., blazars, radio galaxies, Seyfert galaxies, etc.).

The 1FGL catalog includes 216 sources with γ-ray analysis flags and their detection has to be considered carefully since they could have been artifacts of the analysis (Abdo et al. 2010a). In particular, 103 of these 216 1FGL flagged sources have the "c" flag following the 1FGL name; this indicates that the source is found in a region with bright and/or possibly incorrectly modeled diffuse emission. On the other hand, any non-zero entry in the Flags column indicates inconsistencies found during the analysis (see Abdo et al. 2010a, for details). However, we note that 36 out of 103 "c"-flagged 1FGL sources are also detected in 2FGL, and only 25 of them were still indicated with a "c" flag therein. Thus, we decided to keep all of the c-flagged sources in our analysis since they could be useful for reference in future releases of *Fermi* catalogs.

3.2. The Fermi-LAT Second Source Catalog

The 2FGL catalog,[14] based on 24 months of *Fermi* operation, lists 1873 γ-ray sources (Nolan et al. 2012). This catalog includes the following:

1. 108 PSRs, 25 associated plus 83 identified;
2. 3 PWNs, all three identified;

[14] http://fermi.gsfc.nasa.gov/ssc/data/access/lat/2yr_catalog/

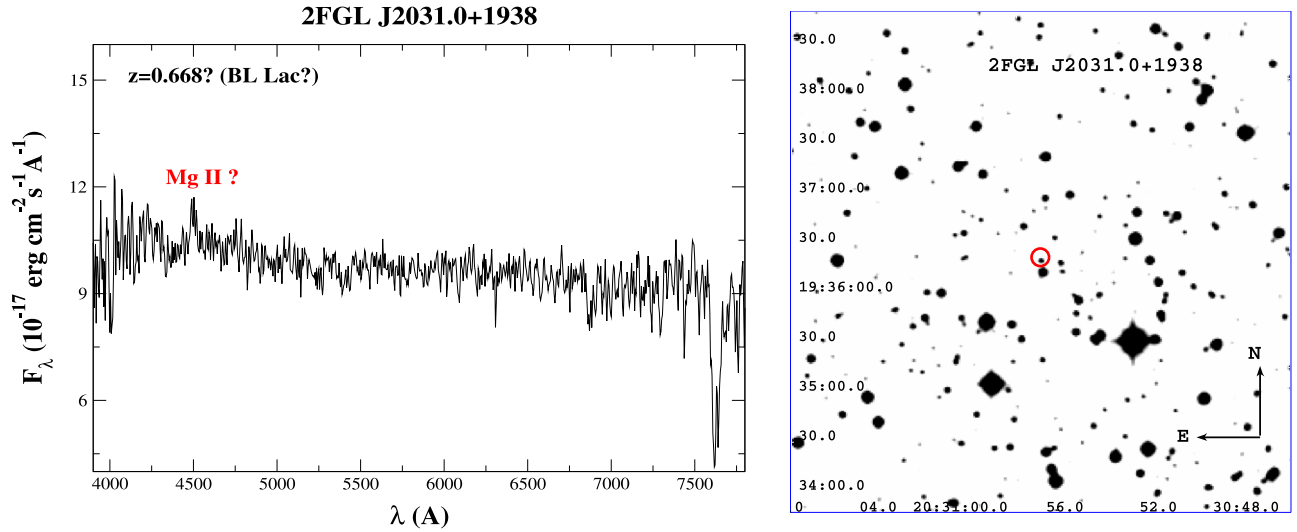

Figure 14. (Upper panel) Optical spectra of the counterpart associated with 2FGL J2031.0+1938 observed at OAN in San Pedro Mártir (México) on 2014 July 1. The emission line potentially identified as Mg I is marked. The source has been classified as a BL Lac. (Lower panel) 5′ × 5′ finding chart from the Digitized Sky Survey (red filter). The potential counterpart of 2FGL J2031.0+1938 is indicated by the red circle.

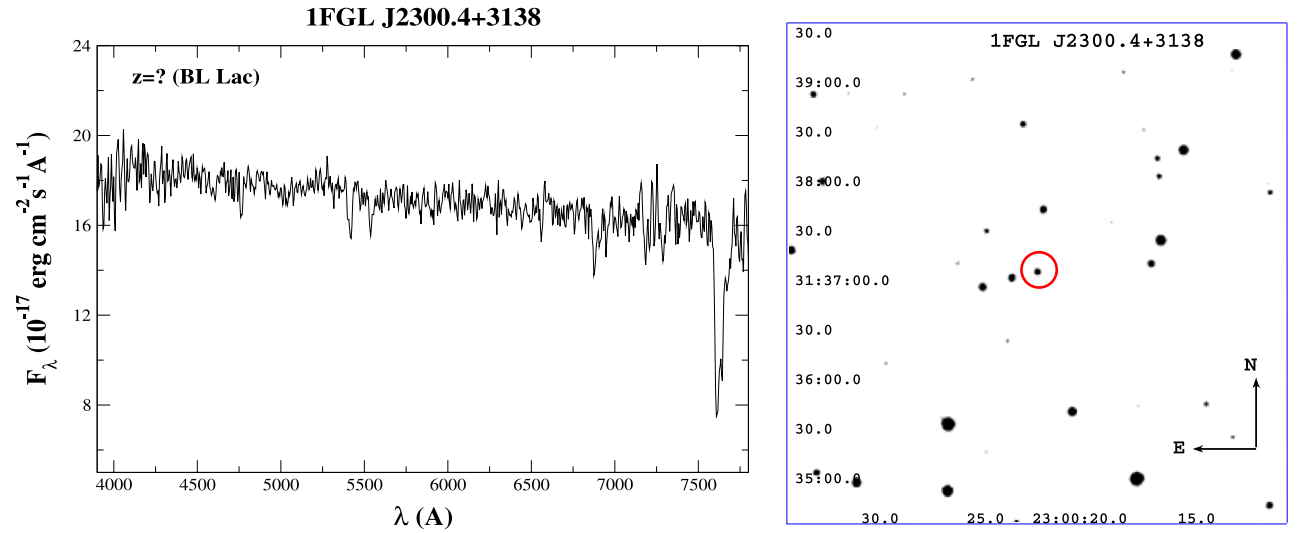

Figure 15. (Upper panel) Optical spectra of the counterparts associated with 2FGL J2300.4+3138 observed at OAN in San Pedro Mártir (México) on 2014 July 1. Several unidentified absorption features superimposed to the optical continuum are visible; however, we were not able to identify the C IVfeature previously reported by Shaw et al. (2013a). (Lower panel) 5′ × 5′ finding chart from the Digitized Sky Survey (red filter). The potential counterpart of 1FGL J2300.4+3138 pointed during our observations is indicated by the red circle.

3. 61 γ-ray sources corresponding to 50 SNRs, 55 associated plus 6 identified; and
4. 11 associated GLC, 4 HMB, all identified and 1 nova (NOV),

among the Galactic sources, while in the extragalactic sky there are the following:

1. 435 BZBs, only 7 identified;
2. 370 flat spectrum radio quasars (BZQs), 17 identified;
3. 11 non-blazar-like AGNs, 1 identified;
4. 257 AGNs of uncertain type (AGUs);
5. 6 normal galaxies and 4 starburst galaxies.

The remaining 577 *Fermi* sources were are all UGSs.

The 2FGL catalog *lists* 472 sources with γ-ray analysis flags,155 of which of also have the "c" flag following the 2FGL name. It is also worth noting that with respect to the 1FGL catalog, the fraction of UGSs decreased from 630 out of 1451 sources (~43%) to 577 out of 1873 (~31%) in 2FGL.

4. INTRODUCING THE CLASSIFICATION FOR THE LOW-ENERGY COUNTERPARTS OF THE *FERMI* SOURCES

We adopt the following class definitions for Galactic counterparts of the *Fermi* sources summarized in Table 2: HMB, GLC, nova (NOV), millisecond pulsar (MSP), PSR, PWN, SNR, SFR, and binary star (bin). The classes that we assign for extragalactic counterparts are BZB, quasar radio loud of flat spectrum type (BZQ), blazar of uncertain type (BZU), radio galaxy (rdg), normal galaxy (gal), starburst galaxy (sbg), and Seyfert galaxy (sey). We note that we used three-letter designators to indicate the class for each counterpart; these are shown in lower case to differentiate them from the acronyms

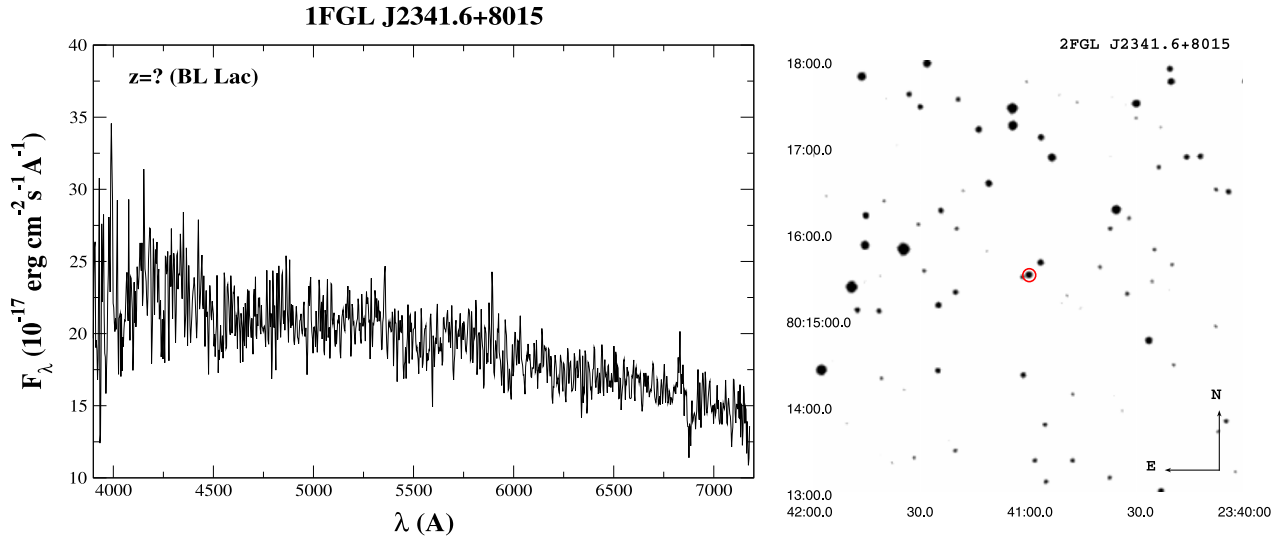

Figure 16. (Upper panel) Optical spectra of the counterparts associated with 1FGL J2341.6+8015 observed at OAGH on 2014 August 28. The source has been classified as a BL Lac on the basis of its featureless continuum. (Lower panel) $5' \times 5'$ finding chart from the Digitized Sky Survey (red filter). The potential counterpart of 1FGL J2341.6+8015 is indicated by the red circle.

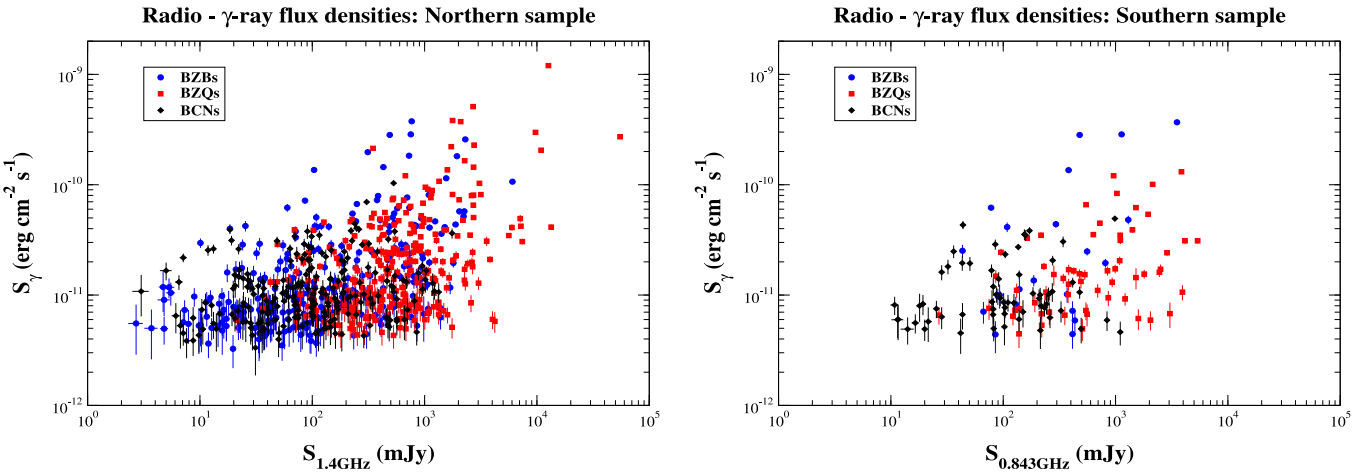

Figure 17. Scatter plot of the radio flux densities vs. the γ-ray flux for blazar-like sources. Spectroscopically confirmed BZBs and BZQs are shown in blue circles and red squares, respectively, while BCN sources are black diamonds. Sources with a radio counterpart in NVSS are in the upper panel while the sources in SUMSS are in the lower panel.

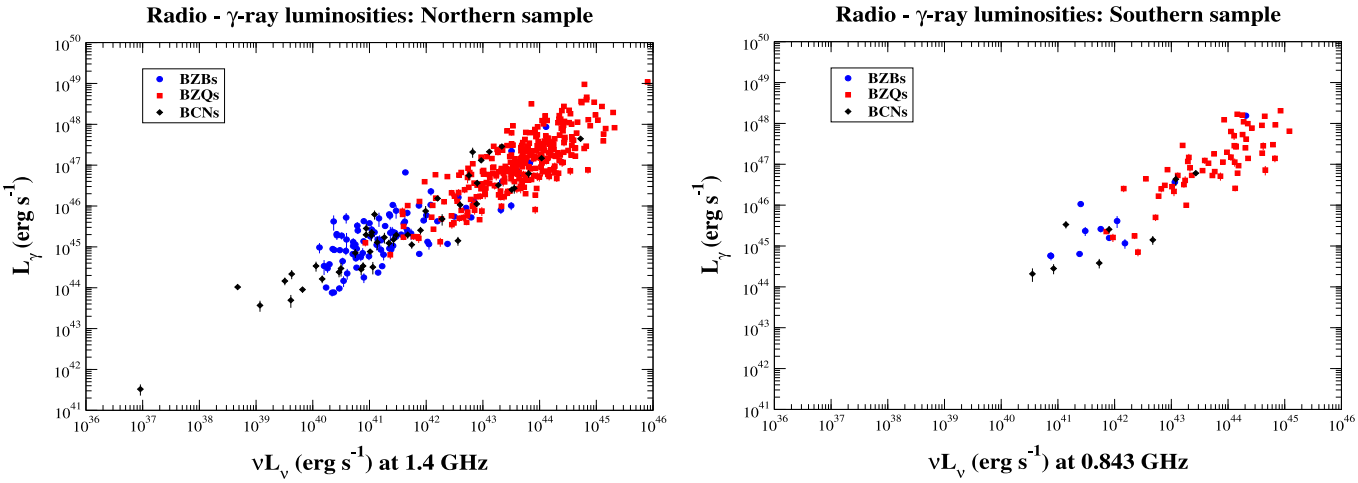

Figure 18. Scatter plot of the radio–γ-ray luminosities for blazar-like sources. Spectroscopically confirmed BZBs and BZQs are shown in blue circles and red squares, respectively, while BCNs sources are black diamonds. Sources with a radio counterpart in the NVSS are in the upper panel while the sources in SUMSS are in the lower panel.

used throughout the paper (see Table 1). We emphasize that the labels used for the extragalactic blazar subclasses are used only if the counterpart corresponds to a source classified in the Roma-BZCAT(Massaro et al. 2009, 2011b). We used version 4.1 of the Roma-BZCAT in our analysis. We also emphasize that the proposed classification depends on the availability of the optical spectroscopic information for the low-energy counterparts.

We also considered BCN as a counterpart class to indicate sources having at least one of the following requirements: (1) being classified as a BL Lac candidate in Roma-BZCAT; (2) belonging to the Combined Radio All-Sky Targeted 8 GHz Survey radio catalog (CRATES; Healey et al. 2007) with a BL Lac-like or a quasar-like *optical* spectrum available in the literature; (3) radio sources with a blazar-like optical spectrum available in literature (i.e., a published spectrum or a description of the features found in the near-IR–optical band) and with a WISE counterpart.

Finally, we labeled as unclassified counterparts (unc) those sources satisfying at least one of the following criteria: (1) WISE IR colors similar to those of γ-ray blazars selected according to the association methods developed by D'Abrusco et al. (2013) and/or with the kernel density estimator (KDE) analysis (Massaro et al. 2012a, 2012c, see also Section 7 for a refined analysis); (2) a flat radio spectrum at frequencies below ~1 GHz (i.e., $\alpha < 0.5$); (3) a radio source with or without an X-ray counterpart associated with the methods adopted in 1LAC and 2LAC; (4) a radio and/or X-ray source that lies at an angular separation between the *Fermi* and counterpart positions smaller than the maximum separation for the blazar class (i.e., 0.°4525 corresponding to 2FGL J1746.0+2316). All of the remaining sources are still unidentified (ugs).

The proposed classification scheme has three main advantages.

1. To have a homogeneous classification of the blazars listed in our analysis and to avoid misclassifications, we adopted the following criterion. We indicate as blazars only those sources that were previously recognized and classified in Roma-BZCAT. There are indeed several counterparts classified as BZB or BZQ listed in the 1LAC and 2LAC catalogs that do not have the same classification according to Roma-BZCAT or for which no optical spectra were found in the literature to confirm their classification.
2. We do not classify a source with a radio and/or X-ray counterpart as an active galaxy of uncertain type (AGU) because these requirements are not strictly sufficient to claim a source as an AGN or as blazar-like, and the lack of multifrequency information does not allow us to determine precisely its nature. Consequently, we introduced the BCN and the unc classes. Once optical spectra and multi-frequency observations become available, a refined classification will be provided.
3. We introduced the SFR class for cases where the *Fermi* position is consistent with a known massive SFR for three reasons. First, to highlight the possibility that an unknown SNR, PWN, and/or PSR is embedded therein, for which multifrequency observations are necessary to confirm their presence. Second, because the use of this information could be adopted to refine γ-ray diffuse models in future releases of the *Fermi* catalogs. In

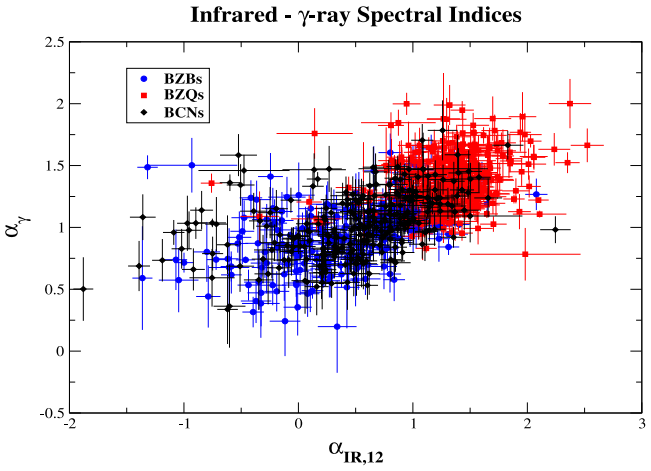

Figure 19. Scatter plot of the infrared spectral index evaluated using the first two WISE bands vs. the γ-ray index for the blazar-like sources in our merged list of refined *Fermi* associations. Spectroscopically confirmed BZBs and BZQs are shown in blue circles and red squares, respectively, while BCN sources are black diamonds.

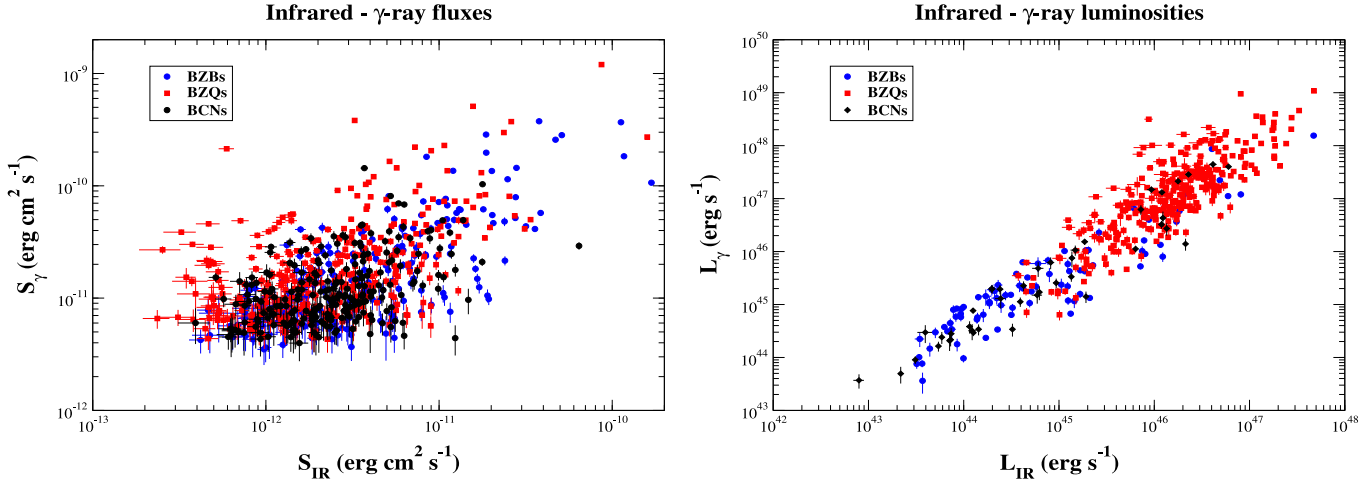

Figure 20. Scatter plot of the infrared-γ-ray fluxes (upper panel) and luminosities (lower panel) for the blazar-like sources. Spectroscopically confirmed BZBs and BZQs are shown in blue circles and red squares, respectively, while BCN sources are black diamonds.

Table 7
Unidentified γ-ray Sources with No Radio Matches and No γ-ray Analysis Flags

1FGL Name	2FGL Name
1FGL J0032.7−5519	2FGL J0032.7−5521
1FGL J0212.3+5319	2FGL J0212.1+5318
1FGL J0545.6+6022	2FGL J0545.6+6018
1FGL J0709.0−1116	
1FGL J0802.4−5622	2FGL J0802.7−5615
1FGL J0854.6−4504	2FGL J0854.7−4501
1FGL J0933.9−6228	2FGL J0934.0−6231
1FGL J1036.2−6719	2FGL J1036.1−6722
1FGL J1117.0−5339	2FGL J1117.2−5341
1FGL J1306.4−6038	2FGL J1306.2−6044
1FGL J1405.5−5846	
1FGL J1441.8−6404	
1FGL J1518.0−5233	2FGL J1518.4−5233
1FGL J1639.5−5152	
1FGL J1650.3−5410	
1FGL J1702.4−5653	2FGL J1702.5−5654
1FGL J1743.5−3314	
1FGL J1806.2+0609	2FGL J1805.8+0612
1FGL J1825.7−1410c	
1FGL J1948.6+2437	
1FGL J2112.5−3044	2FGL J2112.5−3042
1FGL J2227.4−7804	
1FGL J2325.8−4043	
1FGL J2333.0−5535	2FGL J2332.5−5535
	2FGL J0237.9+5238
	2FGL J1016.4−4244
	2FGL J1058.7−6621
	2FGL J1208.5−6240
	2FGL J1404.0−5244
	2FGL J1410.4+7411
	2FGL J1422.3−6841
	2FGL J1507.0−6223
	2FGL J1617.3−5336
	2FGL J1626.4−4408
	2FGL J1639.8−5145
	2FGL J1641.8−5319
	2FGL J1643.3−4928
	2FGL J1741.1−6750
	2FGL J1742.5−3323
	2FGL J1753.8−4446

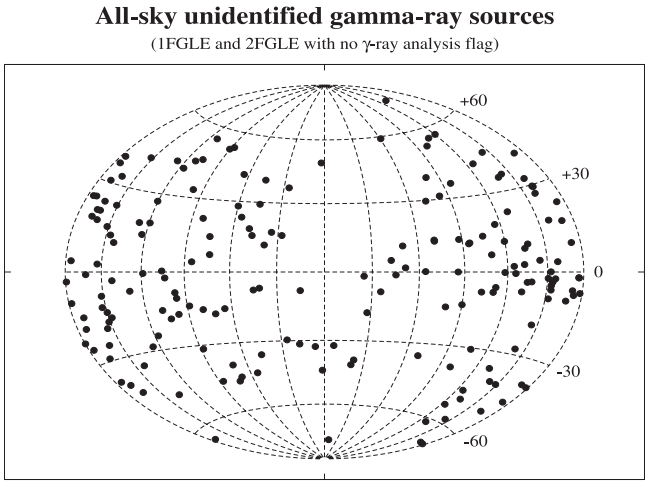

Figure 21. All-sky distribution of the remaining UGSs with no γ-ray analysis flags in the refined association list of the *Fermi* catalogs.

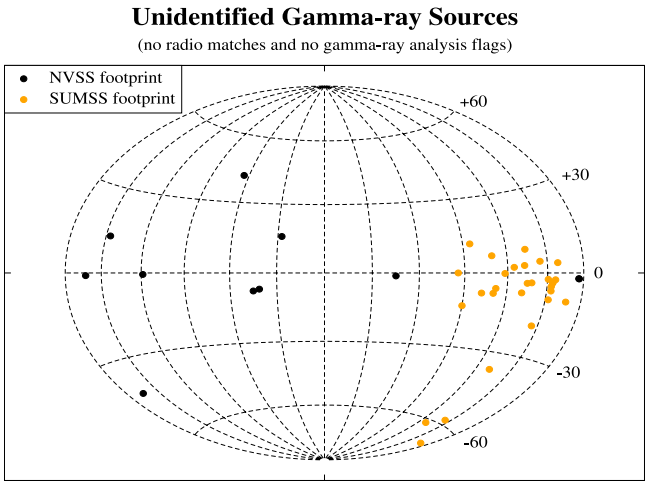

Figure 22. All-sky distribution of the 40 UGSs that do not have any NVSS and/or SUMSS radio source within their positional uncertainty regions at 95% level of confidence and do not present any γ-ray analysis flag. We show those lying in the NVSS footprint (i.e., decl. greater than −40°) as black circles while the others in the Southern hemisphere are indicated as orange circles.

particular, the largest fraction of these SFR potential associations were determined using the recent WISE Catalog of Galactic H II Regions[15] (Anderson et al. 2014), which was not available during the preparation of the currently published *Fermi* catalogs. This could also reveal new correspondences between the uncertainties of the diffuse γ-ray background models and regions of interstellar medium in the Galactic plane. Third, this could be useful for future investigations of the environments of Galactic γ-ray sources.

Finally, we note that for the sources indicated as candidate associations and classified as SFRs, SNRs, PWNs, and PSRs, we investigated the radio and IR images available in NVSS, the Westerbork Synthesis Radio Telescope (WSRT) Galactic Plane Compact 327 MHz Source Catalog (WSRTGP; Taylor et al. 1996), the Molonglo Galactic Plane Survey[16] (MGPS; Green et al. 1999) catalogs, and in the WISE archives, searching for signatures of potential γ-ray emitters.

In Figures 1 and 2, we show two cases of γ-ray sources that have extended structures associated with an open star cluster in an SFR found within their *Fermi* positional uncertainty regions. These are two examples of star clusters where some members could have progressed to become a PSR, PWN, and/or an SNR, and so are plausible counterparts for the γ-ray emission.

Then, in Figures 3 and 4, we report the two best cases of SFRs for which a signature of a shell-like or ring-like extended structures was found within the *Fermi* positional uncertainty region which could be ascribed as a shock signature potentially responsible for the γ-ray emission.

[15] http://astro.phys.wvu.edu/wise/

[16] http://www.astrop.physics.usyd.edu.au/MGPS/

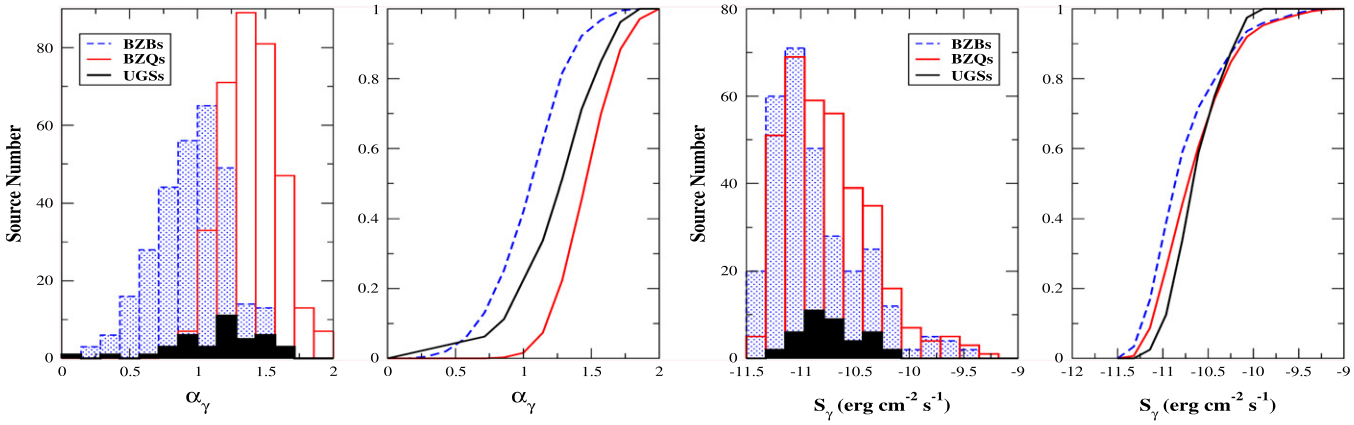

Figure 23. Distribution of the γ-ray spectral index (top) and that of the energy flux (bottom) for the 40 UGSs (straight black line) that do not have any NVSS and/or SUMSS radio source within their positional uncertainty regions and without γ-ray analysis flags in comparison with those of BZBs (dashed blue line) and BZQs (straight red line). Cumulative distributions are also reported in the right panels. The energy flux is the one reported in both the 1FGL and the 2FGL catalogs.

5. CORRELATION WITH EXISTING DATABASES

We searched the following major radio, IR, optical, and X-ray surveys and both the NASA Extragalactic Database (NED)[17] and the SIMBAD Astronomical Database[18] to verify whether multifrequency information can confirm the natures of uncertain counterparts and BCN. In the following, we list all of the catalogs and the surveys searched for our investigation; the abbreviations correspond to the designators used for the multifrequency notes in Table 4.

Below ∼1 GHz radio frequency, we searched the VLA Low-Frequency Sky Survey Discrete Source Catalog (VLSS; Cohen et al. 2007,—V) and the recent revision VLLSr[19] (Lane et al. 2014), both the Westerbork Northern Sky Survey (WENSS; Rengelink et al. 1997,—W) and the Westerbork in the Southern Hemisphere Source Catalog (WISH; De Breuck et al. 2002,—W), the SUMSS(Mauch et al. 2003,—S), the Parkes-MIT-NRAO Surveys (PMN; Wright et al. 1994,—Pm), the Texas Survey of Radio Sources at 365 MHz (TEXAS; Douglas et al. 1996,—T), the Parkes Southern Radio Source catalog (PKS; Wright & Otrupcek 1990,—Pk),and the Low-frequency Radio Catalog of Flat-spectrum Sources (LORCAT; Massaro et al. 2014a,—L).

For the radio counterparts (i.e., above ∼1 GHz), we searched the NRAO VLA Sky Survey (NVSS; Condon et al. 1998,—N), the VLA Faint Images of the Radio Sky at Twenty Centimeters (FIRST; Becker et al. 1995; White et al. 1997,—F), the 87 Green Bank catalog of radio sources (87GB; Gregory & Condon 1991,—87) and the Green Bank 6 cm Radio Source Catalog (GB6; Gregory et al. 1996,—GB), the Australia Telescope 20 GHz Survey (AT20G; Murphy et al. 2010,—A), the CRATES (Healey et al. 2007,—c), and the Australian Long Baseline Array (LBA) Calibrator Survey of southern compact extragalactic radio sources[20] (LCS1 Petrov et al. 2011,—lcs).

For the IR, we queried the WISE all-sky survey in the AllWISE Source catalog[21] (Wright et al. 2010,—w) and 2MASS (Skrutskie et al. 2006,—M) since each WISE source is automatically matched to the closest 2MASS potential counterpart (see Cutri 2012, for details).

Then, we also searched for optical counterparts, with or without spectra available, in the Sloan Digitized Sky Survey Data Release 9 (SDSS DR9; e.g., Ahn et al. 2012,—s) and in the Six-degree-Field Galaxy Redshift Survey (6dFGS; Jones et al. 2004, 2009,—6). We also queried the United States Naval Observatory (USNO)-B1 Catalog (Monet et al. 2003,—U) for optical counterparts of the BCN and the unc sources and reported their magnitudes since they could be useful to plan future follow up observations. We also verified the presence of an ultraviolet (UV) counterpart in the GALEX GR6 archive[22] (sources with a UV counterpart are marked with a "g" in the notes of Table 4).

In X-rays, we searched the *ROSAT* all-sky survey in both the *ROSAT* Bright Source Catalog (RBSC; Voges et al. 1999,—X) and the *ROSAT* Faint Source Catalog (RFSC; Voges et al. 2000,—X), as well as the *XMM-Newton* Slew Survey (XMMSL; Saxton 2008; Warwick et al. 2012,—x), the Deep Swift X-Ray Telescope Point Source Catalog (1XSPS; Evans et al. 2014,—x), the *Chandra* Source Catalog (CSC; Evans et al. 2010,—x), and the *Swift* X-ray survey for all the *Fermi* UGSs (Stroh & Falcone 2013). We used the same designator for the X-ray catalogs of *XMM-Newton*, *Chandra*, and *Swift*. These X-ray observatories perform only pointed observations, and thus there is the chance that the pointed observations present in their archives and related to the field of the *Fermi* source were not requested as follow up of the γ-ray source but for a different reason. Consequently, the discovery of the X-ray counterpart for an associated and/or identified source could be serendipitous.

To perform the searches over all of the surveys and the catalogs cited above, we considered the 1σ positional uncertainties reported therein, with the only exceptions being the WISE all-sky survey and SDSS DR9. In these two cases, we searched for the closest IR and optical counterparts within a maximum angular separation of 3.″3 and 1.″8 for the AllWISE survey and SDSS DR9, respectively. These values were derived on the basis of the statistical analysis described in D'Abrusco et al. (2013) and Massaro et al. (2014b), developed following the approach also presented in Maselli et al. (2010) and Stephen et al. (2010).

[17] http://ned.ipac.caltech.edu/
[18] http://simbad.u-strasbg.fr/simbad/
[19] http://heasarc.gsfc.nasa.gov/W3Browse/all/vlssr.html
[20] http://astrogeo.org/lcs/
[21] http://wise2.ipac.caltech.edu/docs/release/allwise/
[22] http://galex.stsci.edu/GR6

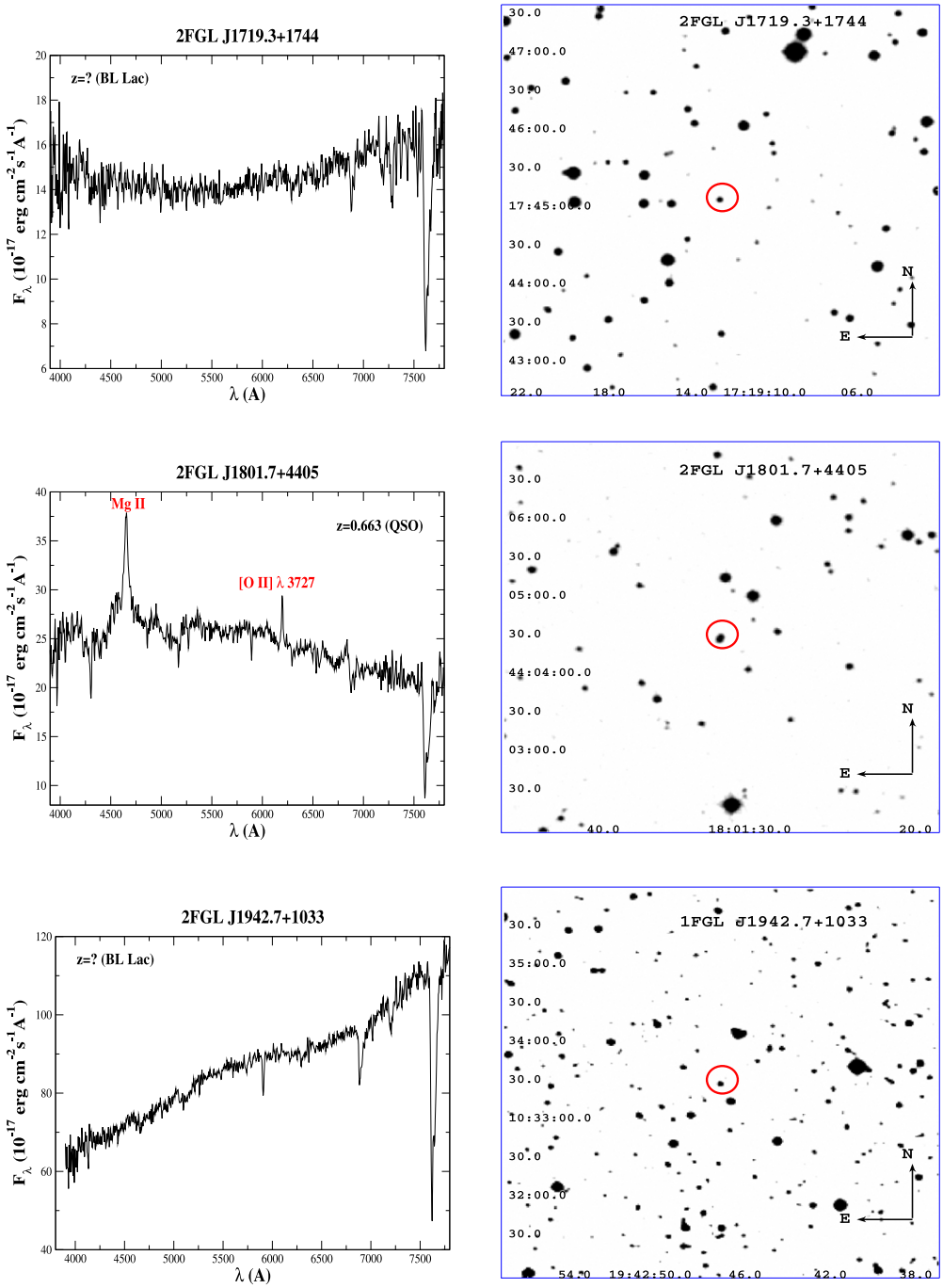

Figure 24. (Upper panel) Optical spectra of the counterparts associated with 2FGL J1719.3+1744, 2FGL J1801.7+4405, and 1FGL J1942.7+1033 already available in literature and re-observed at OAN in San Pedro Mártir (México) on June 29 and 2014 June 30. The Mg II and the [O II] λ3727 emission lines superimposed on the optical continuum are visible in 2FGL J1801.7+4405 and allowed us to classify the source as a quasar, while the lack of features in the other two spectra led toward a BL Lac classification. (Lower panel) $5' \times 5'$ finding chart from the Digitized Sky Survey (red filter). The potential counterpart pointed out during our observations is indicated by the red circle.

To verify the presence of SFRs consistent with the positional uncertainty of the *Fermi* sources, we searched in the following surveys and catalogs: (1) the Sharpless catalog of H II regions (Sharpless 1959), (2) the H II regions in the InfraRed Astronomical Satellite (*IRAS*) point-source catalog (Hughes & MacLeod 1989; Codella et al. 1994), (3) the radio survey of H II regions at 4.85 GHz (Kuchar & Clark 1997), (4) the new catalog of H II regions in the Milky Way (Giveon et al. 2005), (5) the radio catalog of Galactic H II regions from decimeter to millimeter wavelength (Paladini et al. 2003), (6) the SCUBA imaging survey of ultra-compact H II regions (Thompson et al. 2006), (7) the recent WISE Catalog of Galactic H II Regions (Anderson et al. 2014), (8) the QUaD Galactic Plane Survey (Culverhouse et al. 2011), (9) the 5 GHz VLA survey of the Galacitc plane (Becker et al. 1994), and (10) WSRTGP (Taylor et al. 1996). We note that for the cross-matching performed between the SFR catalogs and the *Fermi* sources, we took into account the size of each H II region in combination with the *Fermi* uncertainty position.

To check for the presence of PSRs, we used the Australia Telescope National Facility (ATNF) Pulsar Catalog (Manchester et al. 2005), the Catalog of Galactic SNRs (Green 2009), and the census of high-energy observations of Galactic SNRs[23] (Ferrand & Safi-Harb 2012).

Table 4 summarizes all of the notes derived from the multifrequency analysis. In particular, for the PSRs, we report the information shown in the Public List of LAT-detected γ-ray PSR[24] and by the Pulsar Search Consortium (PSC) as well as from the literature (e.g., Hobbs et al. 2004; Ray et al. 2012, 2013; Pletsch et al. 2012a, 2012b, 2013; Espinoza et al. 2013; Hanabata et al. 2014). Symbols used for their multifrequency notes are labeled as reported in Table 3 (see Abdo et al. 2013, for more details).

6. THE REFINED ASSOCIATIONS FOR THE *FERMI* CATALOGS

The refined associations for the 1FGL and 2FGL catalogs (hereinafter 1FGLR and 2FGLR, respectively) are presented in Table 4. For each source we report the 1FGL name together with those for 2FGL and the 1FHL as derived from the associations published in those catalogs, the counterpart name, and in 37 cases also an alternative association; the category of γ-ray source association; the class of each counterpart as found in the literature; notes derived from the multifrequency investigation; and we also report whether the counterpart lies inside an SFR, and specifically for the PSRs in a PWN or SNR. In addition, in Table 4, we also report if a PWN or SNR contains a known PSR. The coordinates of each counterpart are also included in Table 4 together with the optical magnitudes in the B and R bands from the USNO-B1 Catalog (Monet et al. 2003). Within the multifrequency notes in Table 4, we also indicate if the spectral energy distribution (SED) of the source is shown in Takeuchi et al. (2013), if a redshift estimate is present in the literature (indicating the reference), and if the radio counterpart has a flat radio spectrum (i.e., designated rf in the notes of Table 4 whenever $\alpha < 0.5$ in the radio band). In the online version of the table, we also report the IR analysis flag (Wright et al. 2010) for those sources classified as blazar-like with a counterpart in the AllWISE catalog within 3.″3 as well as the column with the confirmed redshifts.

For the counterpart names we used the following priorities: if the source is a known blazar, then we adopted the Roma-BZCAT nomenclature, and for known pulsars we adopted that of the ATNF Pulsar Catalog[25] (Manchester et al. 2005). Radio galaxies, Seyfert galaxies, and starburst names were indicated based on the Third Cambridge Catalog of Radio Sources and revised versions (3C and 3CR Edge et al. 1959; Bennett 1962; Spinrad et al. 1985), the New General catalog and the Messier catalog, or using their radio names reported in one of the major surveys (see Section 5). Then, Galactic sources such as SNRs and PWNs have their names in Galactic coordinates, as reported in the Catalog of Galactic SNRs[26] (Green 2009), while the most common names were used for GLC and binaries. The counterparts that were associated with SFRs were also labeled with their name in Galactic coordinates. Finally, the remaining uncertain sources were identified by their radio names whenever possible or by their *ROSAT* name. A handful of counterparts were indicated using the nomenclature of optical catalogs. While adopting these choices in the names, we remark that all of the counterparts can be retrieved from the NASA/IPAC Extragalactic Database (NED) and SIMBAD archives without using their coordinates.

6.1. The Refined Associations of the 1FGL

The 1FGLR lists 111 identified sources, 880 associated, 306 candidate associations, and 154 UGSs. The sky distribution of the UGSs is shown in Figure 5 in comparison with the 1FGL associations, in which there were 66 identified objects, 755 associated, and 630 unidentified. The results of our multifrequency analysis for 1FGLR are summarized in Table 5 where we list all of the sources that are identified, associated, and candidate associations for each class separately. We note that the globular cluster GCl 94 (alias M28) associated with 1FGL J1824.5–2449 contains a known MSP PSR J1824–2452A, while 2MASS–GC01 lies in an SFR.

Among the PSRs and the MSPs, there are 21 sources that lie within a known PWN and 4 within SNRs as reported in the notes of Table 4. Twenty PSRs and MSPs out of 39 indicated as candidate associations in both *Fermi* catalogs have been identified after the release of the 2FGL catalog, as presented in the Public List of LAT-detected γ-ray Pulsars. This strongly supports our introduction of this new category of γ-ray sources. In 5 of the 10 associations of PWNs, a PSR has also been found within the nebula and the same situation occurs for 8 SNRs.

We find that 113 1FGL sources have an SFR within their positional uncertainty regions obtained by combining in quadrature the γ-ray localization at a 95% confidence level with the size of the SFR. Three of these sources are HMBs and one is the globular cluster 2MASS–GC01. Fifty six of these 113 have been tentatively associated (i.e., indicated as candidate associations) with previous UGSs, while the remaining *Fermi* objects all have PSRs, PWNs, and/or SNRs embedded in gas clouds and/or interacting with the interstellar medium.[27] Among the 54 candidate associations with SFRs, 2 contain SNRs, 1 a PWN, and 1 a known PSR. However, the potential associations with SFRs could be used to refine the γ-ray Galactic diffuse emission models and the associations in future *Fermi* catalogs, as well as lead to the discovery of new PWNs and/or unknown SNRs. None of the MSPs has been found to lie within a known SFR, but this occurs for 21 PSRs, 7 PWNs, and 18 SNRs.

It is worth noting that 1FGL J0503.2+4526, associated according to the 2FGL and 2LAC analyses with an unclassified source, has as an alternative potential counterpart an SNR that includes a PSR. A similar situation occurs for 1FGL J1837.5–0659c and 1FGL J1846.8–0233c, whose γ-ray emission could be ascribed to a PSR in a PWN. In addition, 1FGL J0622.2+3751 has as an alternative association with a PSR.

Within the unclassified candidate associations (i.e., unc), we noted that eight 1FGLR sources are positionally consistent with SFRs. In addition, we also listed in 1FGLR the tentative association of 1FGL J1653.6–0158 (also known as 2FGL J1653.6–0159) with the binary system that includes PSR J1653–0158 (Romani et al. 2014).

[23] http://www.physics.umanitoba.ca/snr/SNRcat/

[24] https://confluence.slac.stanford.edu/display/GLAMCOG/Public+List+of+LAT-Detected+Gamma-Ray+Pulsars

[25] http://www.atnf.csiro.au/research/pulsar/psrcat/

[26] http://www.mrao.cam.ac.uk/surveys/snrs/

[27] See also http://astronomy.nju.edu.cn/~ygchen/others/bjiang/interSNR6.htm.

Finally, we note that in the extragalactic sky, the SMC (alias NGC 292) is identified with the *Fermi* source 1FGL J0101.3–7257 and is classified as a gal while the LMC is associated with all five of the remaining *Fermi* sources listed as normal galaxies.

6.2. The Refined Associations of the 2FGL

In the analysis of 1FGLR, we have already considered the associations for 1099 *Fermi* sources in common between 1FGL and 2FGL, however, we report the results for all of the refined 2FGL associations (hereinafter 2FGLR) in Table 5. As for 1FGLR, the 2FGLR catalog is dominated by blazar-like sources in the extragalactic sky and by pulsars around the Galactic plane. The 2FGLR lists 126 identified sources as in the original catalog, 1176 associated, 282 candidate associations, and 289 UGSs. The 2FGLR sources are classified as 4 HMB, 11 GLC, 51 MSPs, and 98 PSRs; 21 that lie in a PWN and 6 in an SNR, and 17 associated with an SFR, as indicated in our Table 4. In the case of 2FGLR, among the PSR candidate associations that are not in 1FGLR, only one source has been recently identified according to the Public List of LAT-detected γ-ray Pulsars (see also Abdo et al. 2013). There are also 9 PWNs and 66 sources associated with SNRs, 11 of them with a known PSR lying inside the remnant. We then list 63 *Fermi* sources as candidate associations with SFRs, with 1 also including an SNR. With respect to 1FGL, there is also a new association with an NOV (e.g., Cheung et al. 2014).

The extragalactic sky includes 277 BZBs, 338 BZQs, 54 BZUs, 3 sey, and 3 sbg. Four *Fermi* sources are associated with the γ-ray emission arising from the LMC, as occurred for those objects classified as galaxies in 1FGLR, and one with M31 (i.e., the Andromeda Galaxy; Abdo et al. 2010d). In addition, we find 271 BCN, 320 *Fermi* unclassified sources, and 289 UGSs. In Figure 6, we report the comparison between the sky distributions of all UGSs previously listed in 2FGL and the remaining ones determined in this refined association analysis.

7. IR COLORS OF γ-RAY BLAZAR CANDIDATES AND UNCLASSIFIED SOURCES

As has already been done for the AGUs (Massaro et al. 2012a) and UGSs (e.g., Paggi et al. 2013) listed in 2FGL, we performed a non-parametric analysis of the IR colors for those *Fermi* sources classified as BCN and unc in the merged *Fermi* catalog 1FGLR+2FGLR. We used KDE (see, e.g., D'Abrusco et al. 2009; Laurino et al. 2011 and reference therein) to verify the consistency of their IR colors with the so-called WISE γ-ray Strip (e.g., Massaro et al. 2011a, 2012a, 2013c). The KDE technique allows us to estimate the probability function of a multivariate distribution and does not require any assumption concerning the shape of the "parent" distributions.

Consequently, for all BCN and unc sources with a WISE counterpart, we can provide an estimate of the probability $\pi_{\rm KDE}$ that such a source is consistent with the WISE γ-ray Strip. In particular, we differentiated between $\pi_{\rm KDE,BZB}$ and $\pi_{\rm KDE,BZQ}$ considering the comparison with the IR colors of the BZB and BZQ subclasses, respectively. We considered the Roma-BZCAT blazars listed in both 1FGLR and 2FGLR as training samples to build the WISE γ-ray Strip (Massaro et al. 2011a, 2013a) and to compare the IR colors. We note that the WISE counterparts of the BCN and unc sources with IR analysis flags[28] (Wright et al. 2010) have been considered in our analysis and their flags are reported in Table 4 together with the probabilities derived from the KDE analysis.

In Figure 7, the isodensity contours drawn from the KDE density probabilities are plotted for the *Fermi*-Roma-BZCAT blazars in the [3.4]-[4.6]-[12] μm color–color diagram. The IR colors of the sources listed in the refined association list of the *Fermi* catalogs classified as BCN and unc are also shown. Values of $\pi_{\rm KDE,BZB}$ and $\pi_{\rm KDE,BZQ}$ greater than 5% indicate that the source has IR colors consistent with the portion of the WISE γ-ray Strip constituted by BZBs and BZQs, respectively, at 95% confidence level.

Our analysis confirms that 419 out of 499 total BCN (262) and unc (237) sources in the refined and merged associations list of the *Fermi* catalogs are consistent with the WISE γ-ray Strip at a 95% confidence level. For the unc sources this situation occurs for 172 sources out of 237 objects, while for the BCN it occurs in 242 out of 262 cases. We remark that 374 out of the 499 sources analyzed with KDE are associated, 1 is identified, and the remaining 124 are candidate associations. This analysis supports the introduction of the category of candidate associations, since a large fraction of BCN and unc with a WISE counterpart are likely to be blazar-like sources consistent with the WISE γ-ray Strip.

In our analysis, we took into account the correction for Galactic extinction for all the WISE magnitudes according to the Draine (2003) relation. As shown in D'Abrusco et al. (2013), this correction only marginally affects the [3.4]-[4.6] μm color, mostly at low Galactic latitudes (i.e., 15°).

8. OPTICAL SPECTROSCOPIC OBSERVATIONS OF γ-RAY BLAZAR CANDIDATES

The total number of *Fermi* sources listed uniquely in 1FGLR and 2FGLR are 2219. We found spectroscopic information for 177 which not reported in the previous 1FGL and 2FGL catalogs, including 8 observed during our spectroscopic campaign (see below).

We have been able to confirm spectroscopically 117 BL Lacs, 21 with firm redshift estimates and 27 quasars (QSOs); an additional 8 sources appear to have a BL Lac nature, but the lack of good optical spectra in the literature or, if a spectrum is available, a low signal-to-noise ratio did not allow us to verify their natures. Thus, 24 of these 177 sources still have an uncertain classification and an uncertain redshift estimate. In particular, among these sources we found 11 listed as blazars in Ackermann et al. (2011a) plus 1 listed in Healey et al. (2007) with no optical spectra published or described in the literature. These 177 sources are all listed in Table 4 as BCNs with the exception of one radio source that appears to be an RDG; in the table notes, we report their possible classifications and their redshift estimates with a question mark (?) indicating that further investigation is required.

Optical spectroscopic observations of four candidate associations and of three associated with unclassified sources (unc) were performed with the 2.1 m telescope of the Observatorio Astronómico Nacional (OAN) in San Pedro Mártir (México) on the nights between 2014 June 28 and July 2 (UT) as

[28] As, for example, contamination and confusion from nearby bright sources, see, e.g., http://wise2.ipac.caltech.edu/docs/release/allsky/expsup/sec6_3a.html for additional details.

reported in Table 6. The telescope carries a Boller and Chivens spectrograph and a 1024 × 1024 pixel E2V-4240 CCD. The spectrograph was tuned in the 4000–8000 Å range (grating 300 l mm^{-1}) with a resolution of 4.5 Å per pixel, which corresponds to 8 Å (FWHM), and a 2.″5 slit. Data were wavelength calibrated using Copper–Helium–Neon–Argon lamps, while for flux calibration spectrophotometric standard stars were observed twice during every night of the observing run.

In addition, we also observed the γ-ray blazar candidate BZB J2340+8015 associated with 1FGL J2341.6+8015 at the Observatorio Astrofisico Guillermo Haro (OAGH) located at Cananea, Sonora in México. The telescope was equipped with a Boller & Chivens spectrograph with a CCD SITe 1k × 1k, tuned in the 4000–7000 Å range (grating 150 l/mm). We used a slit width of 2.″5 with a resolution ∼15 Å (FWHM).

The data reduction for both telescopes and instruments was carried out using the IRAF package developed by the National Optical Astronomy Observatory, including bias subtraction, spectroscopic flat fielding, optimal extraction of the spectra, and interpolation of the wavelength solution. All spectra were reduced and calibrated employing standard techniques in IRAF and our own IDL routines (see also Matheson et al. 2008, for additional details).

These eight sources for which new spectroscopic data are provided in our analysis are listed in Table 4 as γ-ray blazar candidates (i.e., BCN). Five of them belong to 1FGLR and are all classified as BZBs according to our analysis; for three of them, the presence of several spectral features allowed us to determine their redshifts. The log of the spectroscopic observations and the results of our analysis are reported in Table 6, while in Figures 8–11 we show their optical spectra together with their finding charts. The remaining three sources are two quasars corresponding to 2FGL J1848.6+3241 and 2FGL J2021.5+0632 as shown in Figures 12 and 13 at redshifts 0.981 and 0.217, respectively, and 2FGL J2031.0+1938, a BZB with an uncertain redshift due to a unique visible emission line, potentially identified as Mg II (see Figure 14).

During our observing nights, we also obtained the spectra for two 2FGL sources, 2FGL J1719.3+1744 and 2FGL J1801.7+4405 (see Figure 24), each with uncertain redshift as reported in Roma-BZCAT (see the figures in the Appendix). We were able to confirm the redshift for 2FGL J1801.7+4405 while 2FGL J1719.3+1744 (alias BZB J1719+1745) is completely featureless. Results for these two additional spectra are also reported in Table 6. We also observed 1FGL J1942.7+1033 (see Figure 24), which is a BZB already classified in the literature (Tsarevsky et al. 2005; Masetti et al. 2013, and Appendix for the figure), and 1FGL J2300.4+3138 for which a series of unidentified absorption features are clearly visible in its optical spectrum. Assuming that these unidentified absorption features are due to Mg II intervening systems along the line of sight, the source should lie at redshift $\geqslant$0.96. This source was in the sample observed by Shaw et al. (2013a), but we cannot confirm their results since we did not find any spectral feature identifiable as C IV (see Figure 15). Finally, we also report the spectrum of BZB J2340+8015 associated with 1FGL J2341.6+8015 observed at OAGH that was originally classified as a BL Lac candidate in Roma-BZCAT at redshift 0.274. We have been able to confirm the BL Lac nature of this source but not its redshift due to its featureless spectrum (see Figure 16). All of our finding charts are from the Digitized Sky Survey.[29]

9. COMPARISON WITH STATISTICAL ANALYSES

We compared our multifrequency analysis on the candidate associations with the results obtained via statistical analyses based on the Classification Tree (CT) and on the Logistic Regression (LR) procedures performed on 1FGL sources (Ackermann et al. 2012) and using the Random Forest algorithm, named *sybil*, presented by Mirabal et al. (2012)[30] for 2FGL sources.

For the 1FGL sources the analysis executed with both the CT and LR statistical methods assesses the probability of correct classification based on the fitting a model form to the *Fermi* data. The result is a PSR-like or AGN-like classification, occurring when the γ-ray source properties are likely to be more consistent with those of a pulsar or an active galaxy, respectively; a similar prediction is also made for the 2FGL sources analyzed by the *sybil* algorithm. Thus, all of these methods provide a classification of the potential counterpart on the basis of the γ-ray properties (e.g., spectral shape, variability, etc) but do not allow us to locate it. Consequently, we can only verify if a candidate association that appears to be a blazar or a pulsar has a corresponding γ-ray source classified as AGN-like or PSR-like by the statistical analyses cited above.

There are 286 type BZB candidate associations in 1FGLR that were analyzed in Ackermann et al. (2012). Within this sample, we found that there is only 1 BZB and 1 HMB, the first statistically classified as AGN-like and the second as PSR-like. Then there are 24 sources classified as BCN, with 23 of them indicated as AGN-like while the last is classified as PSR-like.

Among the Galactic sources, there are the following classifications.

1. Seven sources which we classified as potential MSPs: four appear to be PSR-like while three show γ-ray properties more similar to AGNs (i.e., AGN-like).
2. Twenty-five out of 29 Galactic sources are classified in our analysis as PSRs and are confirmed as PSR-like by statistical methods; meanwhile, four are indicated as AGN-like.
3. Two PWN candidate associations, both resembling PSR-like sources in γ-rays.
4. Five sources reported in our Table 4 as SNRs: four are classified as PSR-like objects and one has an uncertain statistical classification (i.e., indicated as conflict in Ackermann et al. 2012).
5. Thirty-three out of 47 candidate associations are classified as SFRs are PSR-like while only nine appear to be classifiable as AGN-like by the statistical methods; the remaining five are unclassified.

The comparison between our candidate associations in the Galactic plane and the results of the statistical analyses supports the relevance of searching for the presence of SFRs within the *Fermi* positional uncertainty region where PSRs, SNRs, and PWNs could be embedded, or where shocked regions could be potential sources of γ-rays that have not yet been confirmed. Finally, in the sample of 170 unc sources classified as candidate associations in our analysis, 125 appear

[29] http://archive.eso.org/dss/dss
[30] http://www.gae.ucm.es/~mirabal/sibyl.html

to be AGN-like while 40 are PSR-like; the remaining 5 are conflicts between the LR and the CT methods. In particular, four out of eight unc sources that have an SFR consistent with the *Fermi* position are classified as PSR-like on the basis of their γ-ray behavior.

In the case of 2FGLR, we investigated 133 candidate associations with the *sybil* procedure and classified them accordingly. Of these, in the sample of 107 *Fermi* sources that are classified as AGN-like by *sybil*, 24 are BCN and 78 are unc type; the remaining objects are 2 SFRs, 3 PSRs, 7 MSPs (3 expected to be PSR-like γ-ray sources), and 5 SFRs all classified as AGN-like.

Finally, we highlight that the results of the statistical analyses are in agreement with the classification proposed in the refined association lists of both *Fermi* catalogs.

10. γ-RAY CONNECTIONS

10.1. The Radio $\frac{1}{N}$ γ-ray Connection

Many attempts have been made in the past to test for correlations between the radio and γ-ray emission of AGNs and in particular for blazars (e.g., Padovani et al. 1993; Stecker et al. 1993; Salamon & Stecker 1994; Taylor et al. 2007). This connection was also used before the *Fermi* era to search for counterparts of the γ-ray sources (Mattox et al. 1997), thus motivating all of the past and present radio follow-up campaigns for the *Fermi* sources (e.g., Petrov et al. 2013; Schinzel et al. 2014).

However, biases and selection effects have to be taken into account to prove this correlation properly, since it is important to address intrinsic source variability, biases due to redshift dependence (Elvis et al. 1978), the "common distance" bias (Pavlidou et al. 2012), problems related to source misidentifications, and incorrect associations, to name a few. All of these issues can mimic a correlation (Mucke et al. 1997).

Since the launch of *Fermi,* several investigations have also been performed to search for a definitive answer regarding the existence of the radio–γ-ray connection (Ghirlanda et al. 2010, 2011; Mahony et al. 2010) until it was proved and described accurately in Ackermann et al. (2011b). Recently, we also suggested that a link between the radio and the γ-ray emissions in blazars can be extended well below $\sim$1 GHz (Massaro et al. 2013b; Nori et al. 2014; Massaro et al. 2013d).

Given the new multifrequency analysis carried out here and the candidate associations, for the BCN class in particular, we illustrate the current status of the radio–γ-ray connection. To this end, we show both the flux–flux and the luminosity–luminosity scatter plots for the blazars in our merged refined list of *Fermi* associations (see Figures 17 and 18).

A study of the correlations is outside of the scope of this paper. Our main goal is to verify that sources classified as BCN are in agreement with the behavior of blazars in these parameter spaces. It is worth noting that we divided our sample of blazar-like sources into two subsamples: northern and southern samples. The former includes all of the blazars (i.e., BZB, BZQ, and BCN classes) that have a radio counterpart within the NVSS footprint, while in the latter the subsample includes those in the area covered by SUMSS. We distinguish between these two samples since the radio surveys were carried out at different frequencies.

Finally, we remark that only blazars with a firm redshift estimate as reported in our merged list of refined associations are shown in Figure 18. According to this figure, we could expect most of the BCN sources to be BZBs, although this has to be confirmed with optical spectroscopic observations.

10.2. The IR–γ-Ray Connection

D'Abrusco et al. (2012) studied the *Fermi* blazar sample listed in 2FGL and lying in the footprint of the WISE Preliminary survey and reported the discovery of a correlation between their IR and γ-ray spectral indices. This is directly related to their peculiar IR colors and the WISE γ-ray Strip (Massaro et al. 2011a).

Here we report an updated scatterplot for the spectral indices (see Figure 19), as originally presented in D'Abrusco et al. (2012). The correlation between the spectral shapes in the IR and γ-rays is still present and, as occurred in the case of the radio–γ-ray scatter plot (see Section 10.1), the locations of the BCN sources appear to be more consistent with the BL Lac population. The linear correlation coefficient for the whole data set is 0.64. Finally, we also present the connection between IR and γ-ray fluxes and luminosities in Figure 20, which is again in good agreement with our previous results (D'Abrusco et al. 2012, 2013).

11. SUMMARY AND CONCLUSIONS

Two years after the release of the second *Fermi* source catalog, we present a comprehensive multifrequency investigation of all the γ-ray associations listed in both the 1FGL and 2FGL catalogs.

First, we introduced a new category of γ-ray source associations in addition to *identified* and *associated* sources. We label as *candidate associations* those γ-ray sources having a potential low-energy counterpart of a few specific classes of well-known γ-ray emitters lying within the *Fermi* positional uncertainty region and/or with angular separations between the *Fermi* and counterpart positions smaller than the maximum one for all of the associated sources of the same class. Then we provided a new classification scheme for the low-energy counterparts of the *Fermi* sources based on the multifrequency observations and on the optical spectroscopic information now available. We also presented a cross-matching between the *Fermi* catalogs and several surveys of SFRs (see Section 5 for details) to highlight the possibility that an unknown SNR, PWN, and/or PSR is embedded therein, and to provide information that could be used to refine models of diffuse Galactic γ-rays for future releases of the *Fermi* catalogs.

The total number of γ-ray sources considered in our investigation for both 1FGL and 2FGL comprises 2219 unique *Fermi* objects, all listed in Table 4 with each assigned counterpart and their main multifrequency properties. Overall, in the refined association list of the *Fermi* catalogs, we found 174 *Fermi* sources with an SFR consistent with their γ-ray positions. In particular, 60 *Fermi* objects out of these 174 do not have the "c" flag in at least one of the *Fermi* names and include 13 identified sources, 17 associated, and 30 candidate associations. Their counterparts are also classified as 4 HMBs; 17 PSRs, among which 3 lie in a PWN and 2 in an SNR; 3 PWNs, 1 with a PSR; 1 RDG; 13 SNRs, 2 with a PSR included; 1 binary star; 3 unclassified sources; and 19 SFRs.

We found spectroscopic information for 177 extragalactic γ-ray sources not reported in the previous version of the *Fermi* catalogs. We included analyses of 8 new optical spectroscopic observations performed with the 2.1 m telescope of the OAN in San Pedro Mártir and with OAGH to confirm the natures of these blazar-like sources found in our multi-frequency investigation. Blazar candidates and counterparts with unknown origin (i.e., unc) were also analyzed with the KDE technique to determine the fraction that have WISE IR colors similar to known γ-ray blazars. We compared the refined associations listed in both the *Fermi* catalogs with the classification proposed on the basis of statistical investigations (Ackermann et al. 2012; Mirabal et al. 2012) and we found a good agreement with our results.

We note that in the combined list of refined associations for 1FGL and 2FGL, of the 2219 sources, 394 are still UGSs (i.e., ~18% of the entire sample) with 191 having no γ-ray analysis flags. This clean sample of 191 UGSs appears to have a uniform distribution in the sky with a small excess toward the Galactic plane, as shown in Figure 21. Moreover, we conclude that the fraction of *Fermi* sources with plausible counterparts, combining identifications, associations, and candidate associations, within their γ-ray positional uncertainty regions, is ~80% and up to ~90% when considering sources with no γ-ray analysis flags.

Finally, we remark that there are 40 sources (listed in Table 7) within the sample of 191 UGSs that do not have any γ-ray analysis flags that do not have any NVSS and/or SUMSS radio source within their positional uncertainty regions at 95% level of confidence. Their all-sky distribution, separated into those lying in the NVSS footprint (i.e., decl. greater than -40°) and the others observable from the southern hemisphere, is shown in Figure 22. The excess in the subsample of those with decl. less than -40°, clearly visible in Figure 22, could be due to shallower coverage by SUMSS relative to the NVSS catalog. It is worth mentioning that for these 40 UGSs the distributions of the γ-ray spectral index and of the γ-ray fluxes do not show any significant differences from those of BZQs and BZBs (see Figure 23). However, it is intriguing that these UGSs tend to be brighter than the BZB population in γ-rays. It is unlikely that this small ugs subsample is constituted by blazars since, given their γ-ray fluxes S_γ and assuming the typical radio–γ-ray fluxes of the blazar population, the expected radio flux densities should be greater than ~50 mJy for a large fraction, well above the NVSS and SUMSS flux thresholds. On the other hand, we also conclude that their steep values of γ-ray spectral indices are not compatible with sources emitting via dark matter annihilation (e.g., Belikov et al. 2012; Drlica-Wagner et al. 2014).

We thank the anonymous referee for useful comments that led to improvements in the paper. F.M. and G.T. also thank L. Costamante. This investigation is supported by the NASA grants NNX12AO97G and NNX13AP20G. The work by G.T. is supported by the ASI/INAF contract I/005/12/0. H.A.S. acknowledges partial support from NASA/JPL grants RSA 1369556 and 1369565. H.O.F. was funded by a postdoctoral UNAM grant and is currently granted by a Cátedra CONACyT para Jóvenes Investigadores. V.C. acknowledges funding by CONACyT research grant 151494 (México). We thank the staff at the Observatorio Astronómico Nacional in San Pedro Mártir (México) for all their help during the observation runs. Part of this work is based on archival data, software, or online services provided by the ASI Science Data Center. This research has made use of data obtained from the high-energy Astrophysics Science Archive Research Center (HEASARC) provided by NASA's Goddard Space Flight Center; the SIMBAD database operated at CDS, Strasbourg, France; the NASA/IPAC Extragalactic Database (NED) operated by the Jet Propulsion Laboratory, California Institute of Technology, under contract with the National Aeronautics and Space Administration. Part of this work is based on the NVSS (NRAO VLA Sky Survey): the National Radio Astronomy Observatory is operated by Associated Universities, Inc., under contract with the National Science Foundation and on the VLA Low-frequency Sky Survey (VLSS). The Molonglo Observatory site manager, Duncan Campbell-Wilson, and the staff, Jeff Webb, Michael White, and John Barry, are responsible for the smooth operation of Molonglo Observatory Synthesis Telescope (MOST) and the day-to-day observing programme of SUMSS. The SUMSS survey is dedicated to Michael Large, whose expertise and vision made the project possible. MOST is operated by the School of Physics with the support of the Australian Research Council and the Science Foundation for Physics within the University of Sydney. This publication makes use of data products from the Wide-field Infrared Survey Explorer, which is a joint project of the University of California, Los Angeles, and the Jet Propulsion Laboratory/California Institute of Technology, funded by the National Aeronautics and Space Administration. This publication makes use of data products from 2MASS, which is a joint project of the University of Massachusetts and the Infrared Processing and Analysis Center/California Institute of Technology, funded by the National Aeronautics and Space Administration and the National Science Foundation. Funding for SDSS and SDSS-II has been provided by the Alfred P. Sloan Foundation, the Participating Institutions, the National Science Foundation, the U.S. Department of Energy, the National Aeronautics and Space Administration, the Japanese Monbukagakusho, the Max Planck Society, and the Higher Education Funding Council for England. The SDSS Web Site is http://www.sdss.org/. The SDSS is managed by the Astrophysical Research Consortium for the Participating Institutions. The Participating Institutions are the American Museum of Natural History, Astrophysical Institute Potsdam, University of Basel, University of Cambridge, Case Western Reserve University, University of Chicago, Drexel University, Fermilab, the Institute for Advanced Study, the Japan Participation Group, Johns Hopkins University, the Joint Institute for Nuclear Astrophysics, the Kavli Institute for Particle Astrophysics and Cosmology, the Korean Scientist Group, the Chinese Academy of Sciences (LAMOST), Los Alamos National Laboratory, the Max-Planck-Institute for Astronomy (MPIA), the Max-Planck-Institute for Astrophysics (MPA), New Mexico State University, Ohio State University, University of Pittsburgh, University of Portsmouth, Princeton University, the United States Naval Observatory, and the University of Washington. This research has made use of the USNOFS Image and Catalog Archive operated by the United States Naval Observatory, Flagstaff Station (http://www.nofs.navy.mil/data/fchpix/). The WENSS project was a collaboration between the Netherlands Foundation for Research in Astronomy and the Leiden Observatory. We acknowledge the WENSS team consisting of Ger de Bruyn, Yuan Tang, Roeland Rengelink, George

Miley, Huub Rottgering, Malcolm Bremer, Martin Bremer, Wim Brouw, Ernst Raimond, and David Fullagar for the extensive work aimed at producing the WENSS catalog. TOPCAT[31] (Taylor 2005) for the preparation and manipulation of the tabular data and the images. The Aladin Java applet[32] was used to create the finding charts reported in this paper (Bonnarel et al. 2000). It can be started from the CDS (Strasbourg—France), CFA (Harvard—USA), ADAC (Tokyo—Japan), IUCAA (Pune—India), UKADC (Cambridge—UK), or from CADC (Victoria—Canada). We acknowledge the contribution of the JHU Sloan Digital Sky Survey group to the development of this site. Many of its features were inspired by the look and feel of the SkyServer. A special thanks goes to Tamas Budavari for his help with the SDSS–GALEX matching and to Wil O'Mullane for his help with the CASJobs site setup and configuration. We also acknowledge Randy Thompson (MAST) for providing IDL IUEDAC routines and Mark Siebert for providing IDL routines to generate tile JPEG images.

APPENDIX

Here we present the spectra of 2FGL J1719.3+1744 and 2FGL J1801.7+4405, both with uncertain redshift, as reported in Roma-BZCAT together with that of 1FGL J1942.7+1033. We confirmed the redshift for 2FGL J1801.7+4405 and the BL Lac classification of 1FGL J1942.7+1033 (Tsarevsky et al. 2005; Masetti et al. 2013) while 2FGL J1719.3+1744 (alias BZBJ1719+1745) has a completely featureless spectrum.

REFERENCES

Abdo, A. A., Ackermann, M., Ajello, M., et al. 2009, PhRvL, 103, 1101
Abdo, A. A., Ackermann, M., Ajello, M., et al. 2010, ApJS, 188, 405
Abdo, A. A., Ackermann, M., Ajello, M., et al. 2010, ApJ, 715, 429
Abdo, A. A., Ackermann, M., Ajello, M., et al. 2010, ApJ, 723, 649
Abdo, A. A., Ackermann, M., Ajello, M., et al. 2010, A&A, 523, 2
Abdo, A. A., Ajello, M., Allafort, A., et al. 2013, ApJS, 208, 17
Acero, F., Donato, D., Ojha, R., et al. 2013, ApJ, 779, 133
Ackermann, M., Ajello, M., Allafort, A., et al. 2011, ApJ, 743, 171
Ackermann, M., Ajello, M., Allafort, A., et al. 2011, ApJ, 741, 30
Ackermann, M., Ajello, M., Allafort, A., et al. 2012, ApJ, 753, 83
Ackermann, M., Ajello, M., Allafort, A., et al. 2013, ApJ, 209, 34
Ahn, C. P., Alexandroff, R., Allende Prieto, C., et al. 2012, ApJS, 203, 21
Anderson, L. D., Bania, T. M., Balser, D. S., et al. 2014, ApJS, 212, 1
Araudo, A. T., Romero, G. E., Bosch-Ramon, V., & Paredes, J. M. 2007, A&A, 476, 1289
Atwood, W. B., Abdo, A. A., Ackermann, M., et al. 2009, ApJ, 697, 1071
Bade, N., Fink, H. H., Engels, D., et al. 1995, A&AS, 110, 469
Bauer, F. E., Condon, J. J., Thuan, T. X., et al. 2000, ApJS, 129, 547
Baker, J. C., Hunstead, R. W., & Brinkmann, W. 1995, MNRAS, 277, 553
Becker, R. H., White, R. L., Helfand, D. J., & Zoonematkermani, S. 1994, ApJS, 347, 92
Becker, R. H., White, R. L., & Helfand, D. J. 1995, ApJ, 450, 559
Belikov, A. V., Buckley, M. R., & Hooper, D. 2012, PhRvD, 86, 043504
Bennett, A. S. 1962, MNRAS, 125, 75
Berlin, A., & Hooper, D. 2014, PhRvD, 89, 106014
Beuermann, K., Thomas, H.-C., Reinsch, K., et al. 1999, A&A, 347, 47
Bica, E., Dutra, C. M., Soares, J., & Barbuy, B. 2003, A&A, 404, 223
Bikmaev, I. F., Burenin, R. A., Revnivtsev, M. G., et al. 2008, AstL, 34, 653
Bosch-Ramon, V., Romero, G. E., Araudo, A. T., & Paredes, J. M. 2010, A&A, 511, 8
Bonnarel, F., Fernique, P., Bienaymé, O., et al. 2000, A&AS, 143, 33
Britzen, S., Brinkmann, W., Campbell, R. M., et al. 2007, A&A, 476, 759
Cheung, C. C., Donato, D., Gehrels, N., Sokolovsky, K. V., & Giroletti, M. 2012, ApJ, 756, 33
Cheung, C. C., Shore, S. N., & Jean, P. 2014, AAS Meeting Abstracts, 223, 113.01
Codella, C., Felli, M., & Natale, V. 1994, A&A, 284, 233
Cohen, A. S., Lane, W. M., Cotton, W. D., et al. 2007, AJ, 134, 1245
Condon, J. J., Cotton, W. D., Greisen, E. W., et al. 1998, AJ, 115, 1693
Cowperthwaite, P. S., Massaro, F., D'Abrusco, R., Paggi, A., Tosti, G., & Smith, H. A. 2013, AJ, 146, 110
Cutri, R. M., Wright, E. L., Conrow, T., et al. 2013, wise rept, 1
Culverhouse, T., Ade, P., Bock, J., et al. 2011, ApJS, 195, 8
D'Abrusco, R., Longo, G., & Walton, N. A. 2009, MNRAS, 396, 223
D'Abrusco, R., Massaro, F., Ajello, M., et al. 2012, ApJ, 748, 68
D'Abrusco, R., Massaro, F., Paggi, A., et al. 2013, ApJS, 206, 12
De Breuck, C., Tang, Y., de Bruyn, A. G., et al. 2002, A&A, 394, 59
de Ruiter, H. R., Willis, A. G., & Arp, H. C. 1977, A&AS, 28, 211
Del Valle, M. V., & Romero, G. E. 2012, A&A, 543, A56
Doert, M., & Errando, M. 2014, ApJ, 782, 41
Douglas, J. N., Bash, F. N., Bozyan, F. A., Torrence, G. W., & Wolfe, C. 1996, AJ, 111, 1945
Draine, B. T. 2003, ARA&A, 41, 241
Drlica-Wagner, A., Gomez-Vargas, G. A., Hewitt, J. W., Linden, T., & Tibaldo, L. 2014
Drinkwater, M. J., Webster, R. L., Francis, P. J., et al. 1997, MNRAS, 284, 85
Edge, D. O., Shakeshaft, J. R., McAdam, W. B., Baldwin, J. E., & Archer, S. 1959, MmRAS, 68, 37
Elvis, M., Maccacaro, T., Wilson, A. S., et al. 1978, MNRAS, 183, 129
Espinoza, C. M., Guillemot, L., Çelik, Ö, et al. 2013, MNRAS, 430, 571
Evans, I. N., Primini, F. A., Glotfelty, K. J., et al. 2010, ApJS, 189, 37
Evans, P. A., Osborne, J. P., Beardmore, A. P., et al. 2014, ApJS, 210, 8
Ferrand, G., & Safi-Harb, S. 2012, AdSpR, 49, 1313
Ghirlanda, G., Ghisellini, G., Tavecchio, F., & Foschini, L. 2010, MNRAS, 407, 791
Ghirlanda, G., Ghisellini, G., Tavecchio, F., Foschini, L., & Bonnoli, G. 2011, MNRAS, 413, 852
Giommi, P., Polenta, G., Lähteenmäki, A., et al. 2012, A&A, 541A, 160
Giveon, U., Becker, R. H., Helfand, D. J., et al. 2005, AJ, 129, 348
Green, A. J., Cram, L. E., Large, M. I., & Ye, T. 1999, ApJS, 122, 207
Green, D. A. 2009, BASI, 37, 45
Gregory, P. C., & Condon, J. J. 1991, ApJS, 75, 1011
Gregory, P. C., Scott, W. K., Douglas, K., & Condon, J. J. 1996, ApJS, 103, 427
Hanabata, Y., Katagiri, H., Hewitt, J. W., et al. 2014, ApJ, 786, 145
Hassan, T., Mirabal, N., Contreras, J. L., & Oya, I. 2013, MNRAS, 428, 220
Healey, S. E., Romani, R. W., Taylor, G. B., et al. 2007, ApJS, 171, 61
Healey, S. E., Romani, R. W., Cotter, G., et al. 2008, ApJS, 175, 97
Hewett, P. C., & Wild, V. 2010, MNRAS, 405, 2302
Hewitt, A., & Burbidge, G. 1989, in A New Optical Catalog of Quasi-Stellar Objects (Chicago: Univ. Chicago Press)
Hobbs, G., Faulkner, A., Stairs, I. H., et al. 2004, MNRAS, 352, 1439
Hovatta, T., Lister, M. L., Aller, M. F., et al. 2012, AJ, 144, 105
Hovatta, T., Aller, M. F., Aller, H. D., et al. 2014, AJ, 147, 143
Hughes, V. A., & MacLeod, G. C. 1989, AJ, 97, 786
Kataoka, J., Yatsu, Y., & Kawai, N. 2012, ApJ, 757, 176
Kovalev, Y. Y. 2009, ApJL, 707, L56
Kuchar, T. A., & Clark, F. O. 1997, ApJ, 488, 224
Johnston, K. J., Fey, A. L., Zacharias, N., et al. 1995, AJ, 110, 880
Jones, D. H., Saunders, W., Matthew, C., et al. 2004, MNRAS, 355, 747
Jones, D. H., Read, M. A., Saunders, W., et al. 2009, MNRAS, 399, 683
Landoni, M., Massaro, F., Paggi, A., et al. 2014, AJ, submitted
Landt, H., Padovani, P., Eric, S. P., et al. 2001, MNRAS, 323, 757
Lane, W. M., Cotton, W. D., van Velzen, S., et al. 2014, MNRAS, 440, 327
Laurino, O., D'Abrusco, R., Longo, G., & Riccio, G. 2011, MNRAS, 418, 2165
Lister, M. L., Aller, M., Aller, H., et al. 2011, ApJ, 742, 27
López-Caniego, M., González-Nuevo, J., Massardi, M., et al. 2013, MNRAS, 430, 1566
Maeda, K., Kataoka, J., Nakamori, T., et al. 2011, ApJ, 729, 103
Mahony, E. K., Sadler, E. M., Murphy, T., et al. 2010, ApJ, 718, 587
Manchester, R. N., Hobbs, G. B., Teoh, A., & Hobbs, M. 2005, AJ, 129, 1993
Mao, L. S. 2011, NewA, 16, 503
Marti, J., Paredes, J. M., Bloom, J. S., et al. 2004, A&A, 413, 309
Maselli, A., Cusumano, G., Massaro, E., et al. 2010, A&A, 520A, 47
Masetti, N., Sbarufatti, B., & Parisi, P. 2013, A&A, 559A, 58
Massaro, E., Giommi, P., Leto, C., et al. 2009, A&A, 495, 691
Massaro, F., D'Abrusco, R., Ajello, M., Grindlay, J. E., & Smith, H. A. 2011a, ApJL, 740, L48
Massaro, E., Giommi, P., Leto, C., et al. 2011b, Multifrequency Catalogue of Blazars (3rd ed.; Rome, Italy: ARACNE Editrice)

[31] http://www.star.bris.ac.uk/~mbt/topcat/
[32] http://aladin.u-strasbg.fr/aladin.gml

Massaro, F., D'Abrusco, R., Tosti, G., et al. 2012a, ApJ, 750, 138
Massaro, F., D'Abrusco, R., Tosti, G., et al. 2012b, ApJ, 752, 61
Massaro, F., D'Abrusco, R., Paggi, A., Tosti, G., & Gasparrini, D. 2012c, ApJL, 750, L35
Massaro, F., D'Abrusco, R., Paggi, A., et al. 2013a, ApJS, 206, 13
Massaro, F., D'Abrusco, R., Giroletti, M., et al. 2013b, ApJS, 207, 4
Massaro, F., D'Abrusco, R., Paggi, A., et al. 2013c, ApJS, 209, 10
Massaro, F., Giroletti, M., Paggi, A., et al. 2013d, ApJS, 208, 15
Massaro, F., Giroletti, M., D'Abrusco, R., et al. 2014a, ApJS, 213, 3
Massaro, F., Masetti, N., D'Abrusco, R., et al. 2014b, AJ, 148, 66
Massaro, F., Masetti, N., D'Abrusco, R., et al. 2014c, A&A, in press
Mattox, J. R., Schachter, J., Molnar, L., Hartman, R. C., & Patnaik, A. R. 1997, ApJ, 481, 95
Mattox, J. R., Hartman, R. C., & Reimer, O. 2001, ApJS, 135, 155
Matheson, T., Kirshner, R. P., Challis, P., et al. 2008, AJ, 135, 1598
Mauch, T., Murphy, T., Buttery, H. J., et al. 2003, MNRAS, 342, 1117
Maza, J., Wischnjewsky, M., Antezana, R., & González, L. E. 1995, RMxAA, 31, 119
Mirabal, N., & Halpern, J. P. 2009, ApJ, 701, 129
Mirabal, N., Frías-Martinez, V., Hassan, T., & Frías-Martinez, E. 2012, MNRAS, 424, 64
Mirabal, N. 2013, MNRAS, 432, 71
Mirabal, N. 2013, MNRAS, 436, 2461
Mitton, S., Hazard, C., & Whelan, J. J. 1977, MNRAS, 179, 569
Monet, D. G., Levine, S. E., Canzian, B., et al. 2003, AJ, 125, 984
Montmerle, T. 1979, ApJ, 231, 95
Montmerle, T. 2009, in Conf. High-Energy Phenomena in Massive Stars (Spain: Jaen), 14 (arXiv: 0909.0222)
Murphy, T., Sadler, E. M., Ekers, R. D., et al. 2010, MNRAS, 402, 2403
Moskalenko, I. V., Digel, S. W., Porter, T. A., et al. 2007, NuPhS, 173, 44
Mucke, A., Pohl, M., Reich, P., et al. 1997, A&A, 320, 33
Muller, C., Kadler, M., Ojha, R., et al. 2014, A&A, 562A, 4
Nolan, P. L., Abdo, A. A., Ackermann, M., et al. 2012, ApJS, 199, 31
Nori, M., Giroletti, M., Massaro, F., et al. 2014, ApJS, 212, 3
Padovani, P., Ghisellini, G., Fabian, A. C., & Celotti, A. 1993, MNRAS, 260, L21
Paggi, A., Massaro, F., D'Abrusco, R., et al. 2013, ApJS, 209, 9
Paggi, A., Milisavljevic, D., Masetti, N., et al. 2014, AJ, 147, 112
Paladini, R., Burigana, C., Davies, R. D., et al. 2003, A&A, 397, 213
Pavlidou, V., Richards, J. L., Max-Moerbeck, W., et al. 2012, ApJ, 751, 149
Planck Collaboration 2014 A&A, submitted (arXiv:1303.0576)
Petrov, L., Phillips, C., Bertarini, A., Murphy, T., & Sadler, E. M. 2011, MNRAS, 414, 2528
Petrov, L., Mahony, E. K., Edwards, P. G., et al. 2013, MNRAS, 432, 1294
Pletsch, H. J., Guillemot, L., Allen, B., et al. 2012, ApJ, 744, 105
Pletsch, H. J., Guillemot, L., Allen, B., et al. 2012, ApJL, 755, L20
Pletsch, H. J., Guillemot, L., Allen, B., et al. 2013, ApJL, 779, L11
Prestage, R. M., & Peacock, J. A. 1983, MNRAS, 204, 355
Quintana, H., & Ramirez, A. 1995, ApJS, 96, 343
Raiteri, C. M., Villata, M., Carnerero, M. I., et al. 2014, MNRAS, 442, 629
Ray, P. S., Abdo, A. A., Parent, D., et al. 2011, Fermi Symposium proceedings — eConf C110509, arXiv:1205.3089
Ray, P. S., Ransom, S. M., Cheung, C. C., et al. 2013, ApJL, 763, L13
Rengelink, R., Tang, Y., de Bruyn, A. G., et al. 1997, A&AS, 124, 259
Richter, G. A. 1975, AN, 296, 65
Romani, R. W., Filippenko, A. V., & Cenko, S. B. 2014, ApJL, 793, L20
Rowell, G., Horns, D., Uchiyama, Y., et al. 2010, Proc. 25th Texas Symp. on Relativistic Astrophysics, ed. F. M. Rieger (Chair), C. van Eldik, & W. Hofmann (Germany: Heidelberg)
Salamon, M. H., & Stecker, F. W. 1994, ApJL, 430, L21
Saxton, R. D. 2008, A&A, 480, 611
Schinzel, F. K., Petrov, L., & Taylor, G. B. 2014, ApJS, submitted (arXiv: 1408.6217)
Sharpless, S. 1959, ApJS, 4, 275
Shaw, M. S., Romani, R. W., Cotter, G., et al. 2013a, ApJ, 764, 135
Shaw, M. S., Filippenko, A. V., Romani, R. W., et al. 2013b, AJ, 146, 127
Schwope, A., Hasinger, G., Lehmann, I., et al. 2000, AN, 321, 1
Skrutskie, M. F., Cutri, R. M., Stiening, R., et al. 2006, AJ, 131, 1163
Spinrad, H., Marr, J., Aguilar, L., & Djorgovski, S. 1985, PASP, 97, 932
Stephen, J. B., Bassani, L., Landi, R., et al. 2010, MNRAS, 408, 422
Stern, D., & Assef, R. J. 2013, ApJL, 764, L30
Stroh, M. C., & Falcone, A. D. 2013, ApJS, 207, 28
Stecker, F. W., Salamon, M. H., & Malkan, M. A. 1993, ApJL, 410, L71
Stickel, M., & Kuehr, H. 1996, A&AS, 115, 1
Stickel, M., & Kuehr, H. 1996, A&AS, 115, 11
Sutherland, W., & Saunders, W. 1992, MNRAS, 259, 413
Takahashi, Y., Kataoka, J., Nakamori, T., et al. 2012, ApJ, 747, 64
Takeuchi, Y., Kataoka, J., Maeda, K., et al. 2013, ApJS, 208, 25
Taylor, A. R., Goss, W. M., Coleman, P. H., et al. 1996, ApJS, 107, 239
Taylor, G. B., Healey, S. E., Helmboldt, J. F., et al. 2007, ApJ, 671, 1355
Taylor, M. B. 2005, in ASP Conf. Ser. 347, Astronomical Data Analysis Software and Systems XIV, ed. P. Shopbell, M. Britton, & R. Ebert (San Francisco, CA: ASP), 29
Thompson, M. A., Hatchell, J., Walsh, A. J., et al. 2006, A&A, 453, 1003
Thompson, D. J., Djorgovski, S., & de Carvalho, R. 1990, PASP, 102, 1235
Tsarevsky, G., de Freitas Pacheco, J. A., Kardashev, N., et al. 2005, A&A, 438, 949
Titov, O., Jauncey, D. L., Johnston, H. M., et al. 2011, AJ, 142, 165
Titov, O., Stanford, L. M., Johnston, H. M., et al. 2013, AJ, 146, 10
Tody, D. 1986, Proc. SPIE, 627, 733
Vandenbroucke, J., Buehler, R., Ajello, M., et al. 2010, ApJL, 718, L166
Vettolani, G., Cappi, R., & Chincarini, G. 1989
Voges, W., Aschenbach, B., Boller, T., et al. 1999, A&A, 349, 389
Voges, W., Aschenbach, B., Boller, T., et al. 2000, IAUC, 7432R, 1
Warwick, R. S., Saxton, R. D., & Read, A. M. 2012, A&A, 548A, 99
Werner, M., Reimer, O., Reimer, A., & Egberts, K. 2013, A&A, 555A, 102
White, G. L., Jauncey, D. L., Savage, A., et al. 1988, ApJ, 327, 561
White, R. L., Becker, R. H., Helfand, D. J., Gregg, M. D., et al. 1997, ApJ, 475, 479
Wolstencroft, R. D., Savage, A., Clowes, R. G., et al. 1986, MNRAS, 223, 279
Wright, A., & Otrupcek, R. 1990, PKS Catalog, 0
Wright, A. E., Griffith, M. R., Burke, B. F., & Ekers, R. D. 1994, ApJS, 91, 111
Wright, E. L., Eisenhardt, P. R. M., Mainzer, A. K., et al. 2010, AJ, 140, 1868
Zechlin, H.-S., Fernandes, M. V., Elsässer, D., & Horns, D. 2012, A&A, 538A, 93